THESIS

THE EFFECTS OF WILDFIRE ON TREE TEMPERATURES AND TREE WELL DEVELOPMENT IN THE SEASONAL SNOW ZONE

Submitted by

Erika Lee

Department of Ecosystem Science and Sustainability

In partial fulfillment of the requirements

For the Degree of Master of Science

Colorado State University

Fort Collins, Colorado

Summer 2025

Master's Committee:

Advisor: Stephanie Kampf

Daniel McGrath
David Barnard

ABSTRACT

THE EFFECTS OF WILDFIRE ON TREE TEMPERATURES AND TREE WELL DEVELOPMENT IN THE SEASONAL SNOW ZONE

The western United States is experiencing unprecedented increases in wildfire activity in mountainous regions. Some of these fires are burning high elevation watersheds of the Rocky Mountains, impacting downstream water quality and availability for both ecosystems and human use. Wildfires can affect the magnitude of snow accumulation and timing of snow melt in these ecosystems, causing earlier peak runoff and extended periods of drought. Prior research on energy budget changes after a wildfire have predominantly focused on altered shortwave radiation and the resulting consequences for the snowpack, but little is known about how the darker tree surfaces of burned trees alter radiation and snow processes in a wildfire-impacted forest. This study quantified how temperatures of burned trees compared to those of unburned, live trees during the snow season in the Cache la Poudre River Watershed in Northern Colorado. This study also analyzed the tree well development and resulting snow melt rates around burned trees compared to open regions. My results showed that burned trees had surface temperatures 2.9–7.3 °C warmer, on average, than live trees during daytime hours. At night, burned trees' surface temperatures were 1.8–4.7 °C cooler than live trees. Tree wells developed and persisted primarily during the peak ablation period in the spring, when the average tree surface temperature remained above freezing and snow depth and snow water equivalent (SWE) decreased from day to day. For a given date, the size of the tree trunk was strongly correlated

with tree well diameter (mean R^2 value of 0.78), and over the peak ablation season, the cumulative tree surface temperature strongly correlated with well diameter (mean R^2 value of 0.82). Snow melt volume calculations revealed that the area directly surrounding burned trees had a daily mean of 38% less snow than an open area of the same size during peak ablation. The snow melted 64% faster, on average, around trees than in open areas, resulting in a mean snow-free date 13 days earlier directly next to burned trees compared to open regions.

These results indicate that tree surface temperature plays a critical role in the total radiation budget of a burned forest. The lack of canopy and increased shortwave radiation coupled with char on burned tree surfaces drives the increase in surface temperature, resulting in more longwave radiation emitted from burned tree trunks during the day. This longwave radiation melts the snow surrounding the trees to create tree wells. Further analyses of wildfire's impact on snowpack and water availability should consider the cumulative influence of longwave radiation from burned trees on the snow energy budget and resulting melt rates. This information will help to improve snow energy budget and snowmelt runoff models, providing critical improvements in water planning and management throughout regions of the west that rely on snow as a primary water source.

ACKNOWLEDGEMENTS

I would like to thank everyone who provided guidance throughout my time in graduate school and for this research project. First and foremost, I am deeply grateful to my advisor, Stephanie Kampf, for her constant encouragement and guidance throughout the winding path that my research took. Thank you to my committee, Dan McGrath and Dave Barnard, along with the NSF project team, for their knowledge and productive feedback. Thank you to my entire lab group for the assistance with data collection and maintaining field equipment; Megan Sears, Kira Puntenney-Desmond, Clara Mosso, Joseph Grimley, Sushma Tiwari, and Will Keenan. And to all my fellow peers that donated their time to assist with field work, this research would not have been possible without your help. I am thankful to have received funding for this research from the National Science Foundation, USDA Agricultural Research Service (ARS) and Colorado Mountain Club.

To all my friends and community that supported me personally in the process of reentering academia, with extra gratitude to Abby McNamara – thank you for reaffirming my commitment to this goal. I am profoundly appreciative of my family for their endless encouragement and support. I would not be where I am today without them. A special note of gratitude to Josh Horner for the unlimited use of his power tools and all the time he gave to supporting me throughout graduate school.

My research took place on the ancestral homelands of the Arapaho, Cheyenne and Ute Nations. I am grateful to have the privilege to conduct research in this area and acknowledge the unceded status of this land as important context to my work. I hope that in some way these

research findings will support the protection of and reverence for this small, but important, area of the southern Rocky Mountains.

TABLE OF CONTENTS

ABSTRACT ii
ACKNOWLEDGEMENTS iv
1. INTRODUCTION 1
1.1 Background Information 1
1.2 Research Objectives and Questions 4
1.2.1 Tree Surface Temperature 4
1.2.2 Well Development 5
1.2.3 Snow Volume and Melt Rate Comparison 6
2. METHODS 7
2.1 Site Description 7
2.2 Experimental Design 7
2.3 Data Collection and Analysis 10
2.3.1 Tree Surface Temperature 10
2.3.2 Well Development 12
2.3.3 Melt Rate Comparison 16
3. RESULTS 19
3.1 Tree Surface Temperature 19
3.2 Well Development 29
3.3 Melt Rate Comparison 34
4. DISCUSSION 38
4.1 Snow Energy Balance 38
4.1.1 Tree Temperature 38
4.1.2 Tree Wells 41
4.2 Snow Melt Rates 42
4.3 Temporal and Spatial Context 48
4.4 Project Limitations 49

4.4.1 Study Area 49
4.4.2 Well Development and Snow Volume Calculations 50
5. CONCLUSION 51
REFERENCES 53

1. INTRODUCTION

1.1 Background Information

In the Rocky Mountains of Colorado, over 60% of annual precipitation falls as snow (Serreze et al., 1999). As winter ends, snow melts and turns into streamflow, generating about 80% of the annual water for Colorado (Barnett et al., 2008). This snowmelt water is potentially threatened by increased wildfire activity in the western United States (Westerling, 2016; Kampf et al., 2022). Some of these fires are burning in high-elevation watersheds of the Rocky Mountains and impacting downstream water quality and availability (Kampf et al., 2022). Such wildfires can affect the amount of snow that persists into the spring, as well as the annual peak snow water equivalent (SWE) (Gleason et al., 2013) by causing snow to melt earlier in the spring. This earlier melt shifts peak runoff timing, potentially lengthening the drought season from midsummer through the fall (Barnett et al., 2005). Decreased snowpack can also reduce water availability to communities downstream. These dynamics highlight the importance of addressing the relationship between wildfires, snowpack depths, and melt rates of forested, snow-covered regions.

When considering the relationship between wildfires, snow depth, and snowmelt rates, the sources of energy initiating snowmelt are critical to understand. In an unburned, snow-covered forest, the sun provides a primary source of energy in the form of incoming shortwave radiation (Hardy et al., 1997). Incoming and outgoing shortwave radiation from snow; longwave radiation from the atmosphere, forest canopy and snow surface; and sensible and latent heat fluxes are other contributing factors to the total energy budget of a forest (Davis et al., 1997;

Seyednasrollah & Kumar, 2014). Disturbances such as wildfires or beetle infestations shift the components of the snowpack surface energy budget. In unburned conditions, the forest canopy & tree trunk play a critical role in the energy budget – canopy cover absorbs and reflects incoming shortwave radiation, and the trees emit longwave radiation from their trunks and branches (Pomeroy et al., 1998; Link & Marks, 1999). In a moderate to high severity burned forest, the shortwave radiation inputs to the snowpack increase and longwave radiation inputs decrease because fewer trees are left standing; char covers parts or all the standing tree surfaces; and the canopy is significantly decreased. These changes lead to more energy being absorbed by the snowpack and earlier snow-free dates post-fire (Wiscombe & Warren, 1980; Gleason et al., 2013). The increase in solar energy absorption by snowpack in burned forests has increased as much as four-fold in wildfire-impacted forests of Colorado, Utah and Wyoming over the past two decades (Gleason et al., 2019).

While the effects of shortwave radiation changes on the snowpack energy budget of burned forests are well documented, the effects of wildfire on longwave radiation fluxes from trees have not yet been studied in detail. In unburned, forested regions where tree trunks are exposed to increased solar radiation, Pomeroy et al. (2009) found that sunlit tree trunks can have temperatures 10 to 20 °C higher than that of local air temperature, leading to enhanced longwave radiation. After fires, trees may warm even more the charred bark has a lower surface albedo, meaning that they absorb more incoming shortwave radiation and convert this to heat. The higher emissivity of char (0.95, on average, compared to 0.7 of live wood) (Kashiwagi et al., 1987), combined with warmer tree surface temperatures, results in a greater increase in longwave radiation emitted by burned trees compared to live trees, depending on the extent of dark char

covering the tree surface. This may, in turn, impact the melt rates of snow directly surrounding charred trees.

In a snow-covered forest, the area surrounding the tree trunk commonly has lower snow depths than the surrounding open area, creating a tree well. In unburned forests, tree wells have primarily been attributed to canopy cover's interception of snow, which reduces the amount of snow reaching the ground below trees (Hardy & Albert, 1995; Davis et al., 1997; Maxwell et al., 2019). Longwave radiation emitted by a tree's canopy and trunk also contribute to well development (Molotch et al., 2007; Molotch et al., 2016), because the radiation can melt the snow surrounding the tree (Musselman & Pomeroy, 2017). A moderate to high severity burned forest has little canopy cover, so canopy interception will have limited effect on tree well development. This lack of canopy cover in a burned forests means that outgoing longwave radiation emitted from tree trunks is likely the primary control on well development around burned trees. The extent of char cover on a burned tree may change the amount a tree warms, thus affecting the longwave radiation emitted.

Other potential drivers of well development include changes the snowpack albedo's albedo inside the tree well and the effects of wind scouring in a burned forest. Gleason et al. (2013) found that char is often deposited around the trunk of a burned tree. This added char on the snowpack decreases snow albedo around trees, leading to increased shortwave radiation absorption and snowmelt directly next to burned trees, which contributes to tree well development. Where trees are exposed to wind scouring in a burned forest, the wind blowing up against the side of the tree may also contribute to well development by scooping out and blowing away some of the snow surrounding the trunk. These wind-developed wells will be asymmetrical due to wind direction primarily impacting the windward side of the tree.

1.2 Research Objectives and Questions

The overall goal of this project is to quantify how surface temperatures of burned trees compare to unburned trees and determine how burning affects tree well development and the resulting snow volume and melt rates around burned trees. This information will help characterize how wildfire impacts the longwave radiation fluxes of a snow-covered, burned forest, and how burned tree's surface temperature and resulting longwave radiation changes snow ablation rates. This project is broken into three parts: i) tree surface temperature, ii) well development and iii) snow volume and melt rate comparison.

1.2.1 Tree Surface Temperature

The extent of char cover on a tree can differ depending on if the trees were living or dead at the time of fire, which dictates their char cover patterns post-fire. For the purpose of this study, trees that were dead at the time of fire are referred to as dead-burn (DB), trees that were living at the time of fire and burned in the fire are green-burn (GB), and trees that are unburned and still living are live trees. DB trees have a darker surface in visible wavelengths, more continuous & deep dark char coverage on all aspects of the trunk, and fewer branches than trees that were alive prior to fire (Figure 1b). GB trees typically have superficial char coverage and a pattern of partial coverage on the tree trunk, which can be aspect-driven due to wind blowing char off the windward side of trees, while the leeward side maintains char (Figure 1a).

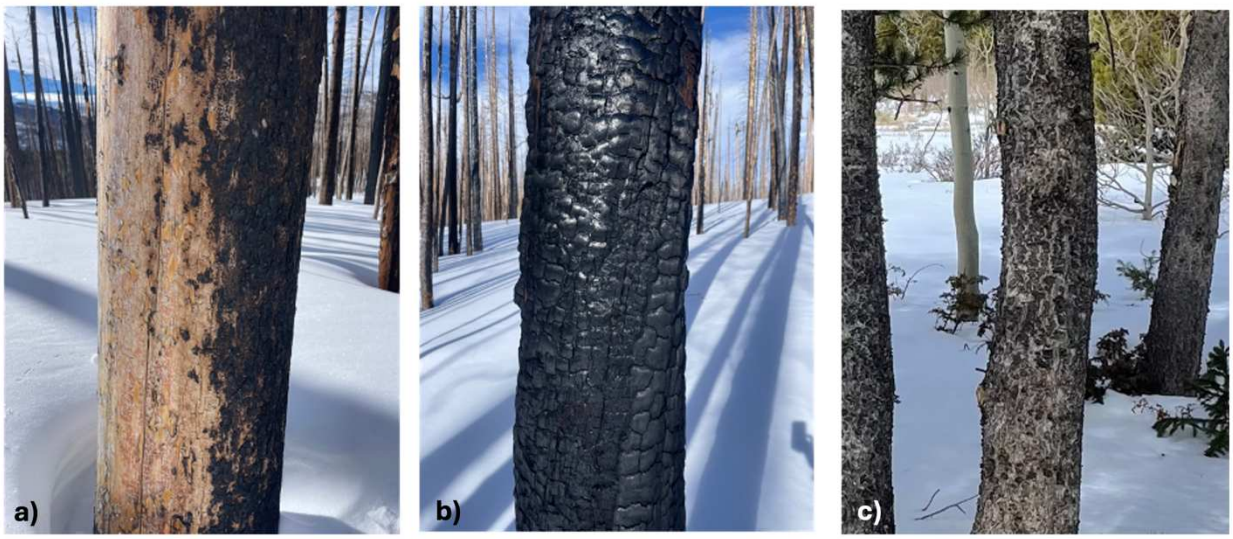

Figure 1. Char pattern and coverage comparison of green-burn (a), dead-burn (b) and live (c) trees from the research area.

The first part of this project investigates whether the tree surface temperatures differ between DB, GB and live trees in two distinct snow zones. Darker objects absorb more shortwave solar radiation than lighter objects and thus warm more during the day (Wiscombe & Warren, 1980), so I hypothesize that a) DB trees, which are covered entirely with char, will have higher mean surface temperatures than GB trees, and b) both DB and GB trees will have higher mean surface temperatures than living trees. Since the total energy radiated is a function of temperature and emissivity, trees with increased surface temperatures and emissivity will also have increased outgoing longwave radiation (Pomeroy et al., 2009).

1.2.2 Well Development

The differences in longwave radiation emitted by trees, which is dependent on the tree surface temperature and emissivity, likely affects the extent of tree well development, the second part of the study. The objective of the well development section of this project is to determine when tree wells develop around burned trees, how their size changes over time, and what factors affect the development of wells. I hypothesized that a) the size of tree wells will be affected by

the size of the tree because larger trees have greater surface areas from which they emit longwave radiation. I also hypothesize that b) the extent of well development will be greater for DB trees than for GB trees, and greater for both burned conditions compared to live trees, due to higher surface temperatures, leading to greater longwave radiation.

1.2.3 Snow Volume and Melt Rate Comparison

The third part of this project aims to quantify and compare the melt rates of areas directly around burned trees to those of open regions. I hypothesize that a) warmer tree surface temperature from burned trees further increases the melt rates of snow next to these trees compared to open areas. This analysis will improve the understanding of tree surface temperature and resulting longwave radiation changes in a burned forest and how this might impact the overall ablation rates of wildfire-impacted forests.

2. METHODS

2.1 Site Description

The study area was located in the Cache La Poudre River watershed in Northern Colorado, west of Fort Collins. This watershed was partially burned during the Cameron Peak Wildfire, which covered approximately 84,500 hectares from August 2020 through December 2020, and was the largest wildfire in Colorado's recorded history (Larimer County, 2021). The study sites included burned and unburned locations in two different snow zones: the persistent snow zone (PSZ) at 3023 meters and the transitional snow zone (TSZ) at 2750 meters (MTBS, 2022) (Figure 2b). The PSZ consists of areas in which snow cover persists through the winter into the spring and where, on average, snow covers the ground for at least 75% of the time from 1 January to 3 July. The TSZ has snow cover present throughout the entire winter and spring, but the snow cover duration changes with elevation. The TSZ is snow covered for 50–75% of the time on average between 1 January and 3 July (Richer et al., 2013; Moore et al., 2014). This selected period encompasses the temporal extend of peak snow accumulation through the entirety of ablation in most parts of the western United States (Hammond et al., 2020). In mountainous regions, lower elevations areas that still receive snow are predicted to have the largest changes in snowpack (Adams et al., 2009). Therefore, I chose to observe both the PSZ and TSZ to compare the burn effects in areas with warmer and colder winter snow conditions.

2.2 Experimental Design

Using National Agricultural Imagery Program (NAIP) imagery (U.S. Department of Agriculture, 2023) along with burn severity (BAER, 2023), bark beetle mortality (Bode et al., 2018; Vorster, 2020), and vegetation type (LANDFIRE, 2020) data, I identified potential study

sites within both snow zones that had similar tree species and burn severity. These locations were then visited in person to choose study sites based on their proximity to weather stations and tree density. The burned sites were primarily composed of lodgepole pine with moderate-high burn severity, while the unburned sites were composed of lodgepole pine and spruce-fir (LANDFIRE, 2020; BAER, 2023). Both burned sites had a mixture of GB and DB trees, with varied tree char coverage patterns, and tree diameters. The DB trees were likely all dead prior to the fire due to bark beetle infestations (Bode et al., 2018; Vorster, 2020). To the extent possible I attempted to locate all the sites on similar slope aspects. The PSZ & TSZ burned sites and the TSZ unburned site aspects are northwest (~315°). The PSZ unburned site aspects is southeast (~150°), but this site has the advantage of being very close to the burned study site. Differences in aspect and tree composition between paired sites were unfortunately unavoidable based on the burn pattern and site access constraints.

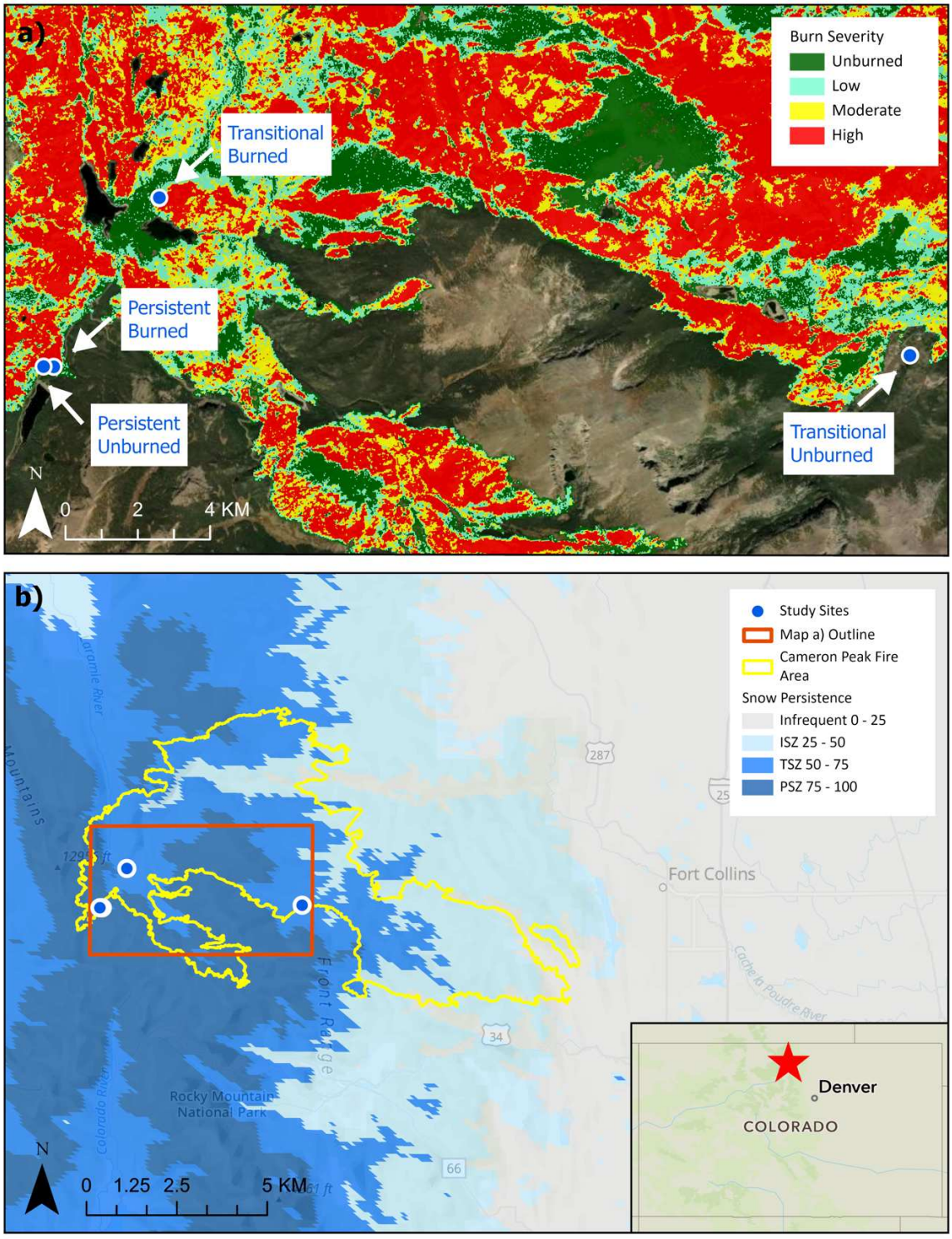

Figure 2. a) Burn severity map with study site locations (blue dots) and b) snow persistence zones with Cameron Peak Fire area (yellow outline) from Hammond (2020) and study site locations, including both weather stations and study areas with sensors (blue dots).

2.3 Data Collection and Analysis

2.3.1 Tree Surface Temperature

To observe the temperature differences between burned and live trees, I monitored both DB and GB trees at the burned sites and live trees at the unburned sites from December 2023 through the snow-free dates of each snow zone, collecting mean temperature data at 15-minute intervals on data loggers (Table 1). Temperature sensors (Campbell Scientific 105-E thermocouple) were placed in 0.02-m deep and 2-m high drill holes in the bark of each tree then secured with ClearWeld professional grade epoxy. One sensor was placed on the north and south sides of each DB, GB and live tree, to investigate whether aspect influenced tree surface temperature (Figure 3, Table 1).

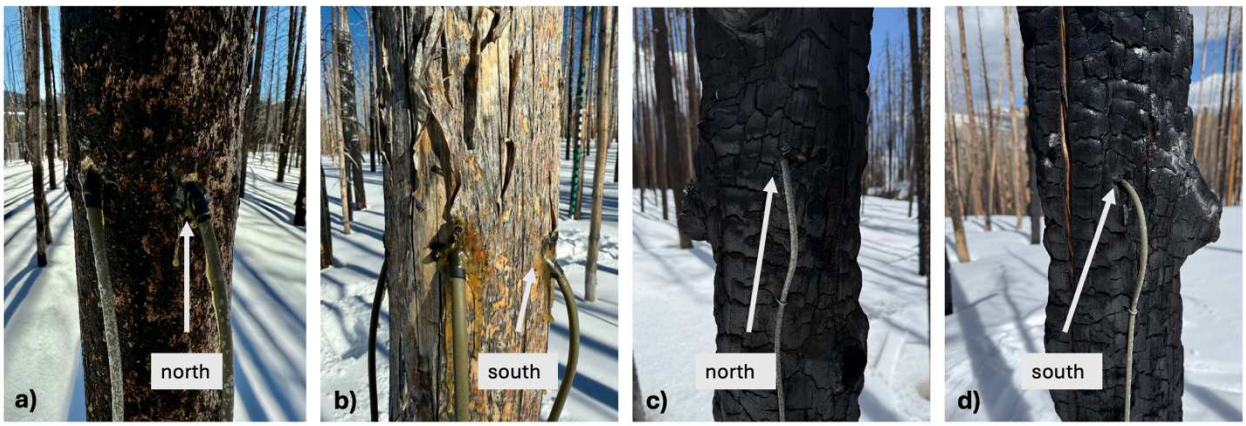

Figure 3. Sensors installed on green-burn and dead-burn trees: a) green-burn north sensor, b) green-burn south sensor, c) dead-burn north sensor, and d) dead-burn south sensor.

Table 1. The model of all data loggers used by site, and quantity, type and aspect of all sensors. All data loggers were manufactured by Campbell Scientific.

Site	Data Logger Model	Total Number of 105E Sensors	Number of Sensors by Burn Condition & Aspect					
			Dead-burn (DB)		Green-burn (GB)		Live	
			North	South	North	South	North	South
Persistent Burned	CR500	8	2	2	2	2	0	0
Persistent Unburned	CR1000	4	0	0	0	0	2	2
Transitional Burned	CR800	8	2	2	2	2	0	0
Transitional Unburned	CR1000	4	0	0	0	0	2	2

Tree surface temperature data was analyzed from 2 February 2024 through the snow-free dates of each snow zone, which represented the longest complete period of tree surface temperature, snow depth, and weather station data for all four sites (PSZ burned/unburned, TSZ burned/unburned). Temperature patterns varied between day and night, so the 15-minute data were separated into day and night intervals using the suncalc R package with day hours accounting for the period from sunrise to sunset (Thieurmel & Elmarhraoui, 2022; R Core Team, 2023).

Our objective in data analysis was to determine if temperatures differed by burn condition. Both snow zones had two replicates of sensors for each of the following tree positions: DB south, DB north, GB south, GB north, live south, live north (Table 1). Due to high correlation between all temperature data, traditional statistical tests could not be run on the data that was collected, so I used a quantitative comparison approach where mean absolute differences of tree surface temperature were calculated to show average comparative trends between burn condition, aspect and day/night temperatures. Using the 15-minute data for each

snow zone, I computed the mean absolute differences for replicates of each tree position from 2 February through the snow-free date of each snow zone. Based on that initial analysis, mean values from the replicate sensors were then compared by the following three factors for the remainder of the analysis: burn condition, aspect and day/night.

2.3.2 Well Development

At each of the PSZ and TSZ burned and unburned sites, 1.5 and/or 3-m snow stakes were installed near one of the trees with temperature sensors. Spypoint Force-20 trail cameras took a photo every 30 minutes, capturing changes in snow depth through the accumulation and ablation season at each snow stake. Data collection began in November 2023 and continued through 6 June 2024, for all cameras. A secondary source of snow depth data was also collected from a trail camera at an unburned location near the TSZ burned site with a more representative snowpack than the location where the TSZ unburned tree temperature sensors were placed; the unburned TSZ site had abnormally low snow accumulation due to high wind scouring. This second TSZ unburned camera gathered data from 1 March–6 June 2024. The trail camera imagery was used to determine maximum snow depths on a daily basis from each 24-hour period, as well as the ablation time period and snow-free dates. I defined the ablation season as starting the day after peak SWE, and the peak ablation period occurring when both the SWE and snow depths were consistently decreasing without any substantial snow accumulation. For all future references, the "accumulation" period includes the beginning of the ablation season up to the start of peak ablation. Snow-free dates were identified for (1) the entire region captured in the trail camera imagery, and (2) individual trees. The snow-free dates for the entire region of observation represented the date in which there was no longer any snow visible on the ground in

the imagery. The snow-free date for the tree areas represented the date that the area surrounding the individual tree no longer had contiguous snow, therefore a well could not be measured.

To evaluate whether tree size increased for larger diameter trees (hypothesis 1.2.2 a) manual tree well surveys were conducted at the TSZ burned site on 12 April and the PSZ burned site on 3 May 2024. During these surveys I measured the tree diameter at breast height (DBH) and well diameter (from east to west) of 13 GB and 5 DB trees at the TSZ burned site and 17 GB and 1 DB trees at the PSZ burned site (Figure 4c). The number and type of trees surveyed at each location was constrained by a lack of DB trees left standing in the sites chosen for this part of the project. To evaluate the effect of tree size, I used Pearson's correlation test in R to compare tree diameter to well diameter from the manual well survey data. The tree diameter is used here because it is easily measured and is related to the surface area of the tree.

To increase the quantity of tree well measurements and gather data for the entire accumulation and ablation period, trail camera images were used to monitor the well sizes of three GB and one DB tree per snow zone at the burned sites (Table 2). This number of GB and DB trees was chosen as it was the most consistent number of trees per burn condition present in the camera imagery across both zones. Because well development in an unburned forest is harder to see with canopy cover obstructing the camera’s views, this assessment was not done for live trees. The images were visually analyzed to assess the timing of well development and see what dates wells were present or had been reset with new snow at each of the four trees. SketchandCalc software was used to collect measurements of the diameter of each tree and well starting on 2 February 2024, once daily through the snow-free dates of each individual tree at both snow zones’ burned sites (SketchandCalc, 2024). Well diameters were measured on a consistent horizontal plane, and tree diameters were measured at the snow-tree horizontal

interface on a daily basis (Figure 4d) to account for vertical variation in tree trunk diameters as the snow melted. Due to how SketchandCalc's online software works, some percent error does exist in measurements (~0.05 m), however this error only exists in where the beginning and end points of the well were defined. Since all SketchandCalc measurements were compared by individual tree, the daily calculations represent a change over time for each tree more than a precise well/tree diameter measurement.

Table 2. Camera imagery analysis tree ID's, burn conditions (dead-burn (DB), green-burn (GB)) and mean tree diameter (m) for the period of observation from February 2nd to the respective snow-free dates of each tree in the persistent (PSZ) and transitional (TSZ) snow zones.

Zone	Tree ID	Burn Condition	Mean Tree Diameter (m)
PSZ	1	GB	0.44
	2	GB	0.18
	3	GB	0.16
	4	DB	0.13
TSZ	1	GB	0.19
	2	GB	0.10
	3	GB	0.08
	4	DB	0.15

To investigate the relationship between tree temperature and well development (hypothesis 1.2.2 b) I computed cumulative values of mean daily tree surface temperature during both the peak ablation period and the accumulation period (including the period of early ablation before peak ablation started), then evaluated whether these values correlated with well diameters from the snow camera data. Cumulative temperature values were used instead of mean or maximum values since well development reflects ongoing input of energy to the snowpack, and temperature is a common proxy used for representing energy available for snowmelt in snow hydrology research (Szeitz & Moore, 2023).

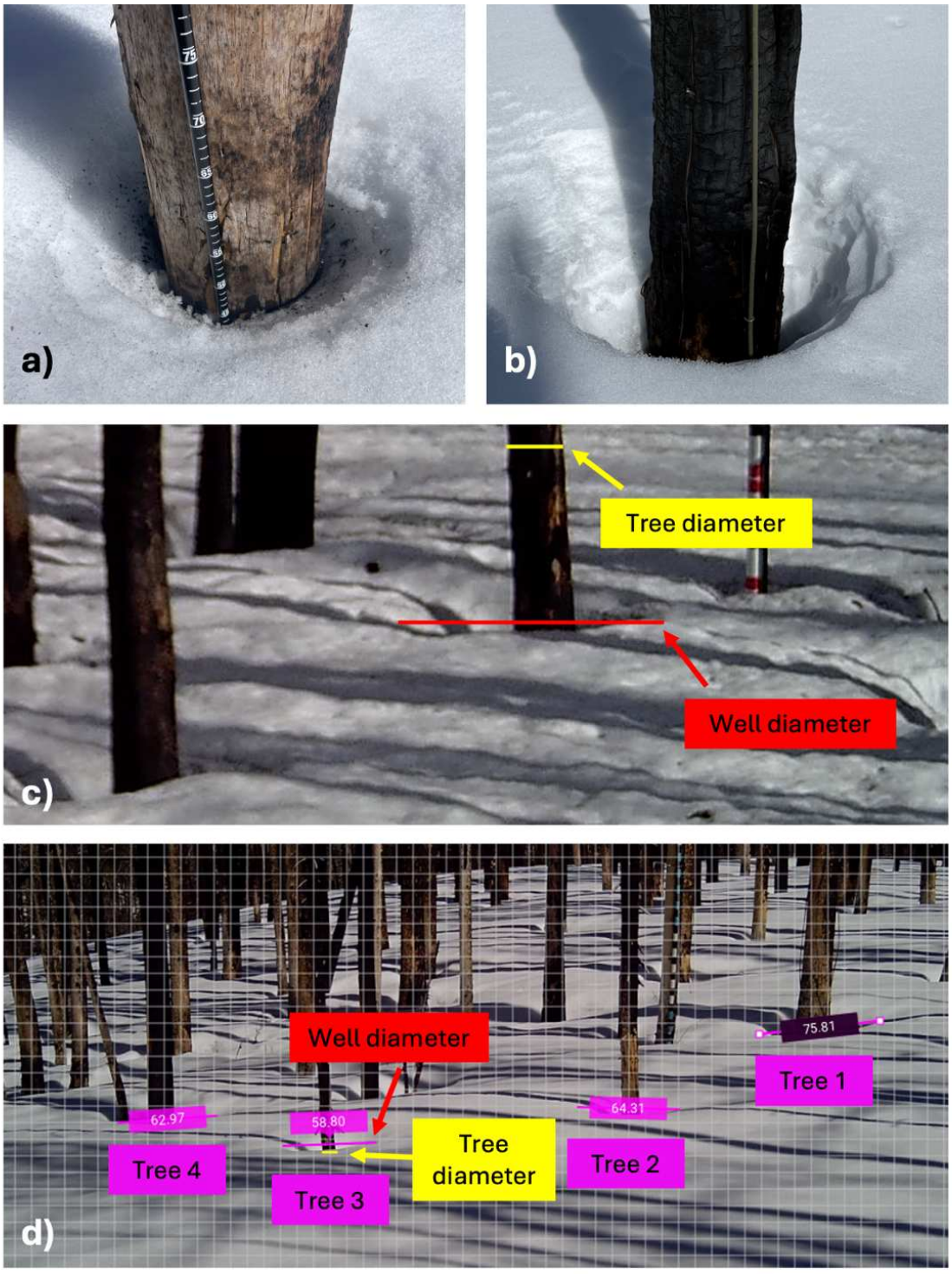

Figure 4. a) well shape noted around a green-burn tree during manual well survey in the transitional snow zone on 12 April 2024, b) observation of well shape around a dead-burn tree and c) a visual of how well and tree diameters were measured from during manual surveys and c) example of SketchandCalc snow camera imagery analysis, showing how tree/well diameters were measured for four trees per site.

2.3.3 Melt Rate Comparison

To test hypothesis 1.2.3 a. and evaluate how tree well development affects overall snowpack melt rates, I compared the snow volume melt rates of the area directly around the four trees observed in the snow camera imagery (Table 2) to that of an open area. I conducted these comparisons for 1.5 m-wide cylindrical shapes surrounding the weather station snow depth sensor compared to the same shape surrounding each of the monitored trees. The 1.5-meter cylindrical shape and size was chosen since it was the largest area not impacted by other trees that encompassed the entire diameter of well development throughout ablation. The snow camera imagery's well diameter and snow depth data were used to compute snow volume around the trees, and sonic distance snow depth sensors (Campbell Scientific SR50-A) were used to determine snow volumes in open areas. The mean daily snow volume was calculated from 2 February 2024 through the snow-free date around each tree and under the snow depth sensors at both the PSZ and TSZ burned sites (Figure 5). I used a half-sphere shape to represent the 3D shape of a tree well. This shape was chosen based on field observation of well shape and the well measurements taken in the manual survey (Figure 4a & b). The following formulas were used to calculate the snow volume around each tree and in the open regions below the snow depth sensors:

$$i) \quad V_t = V_s - V_w \tag{2.1}$$

$$ii) \quad V_s = \pi r_s^2 d_{sc} \tag{2.2}$$

$$iii) \quad V_w = 2/3 \pi r_w^3 \tag{2.3}$$

$$iv) \quad V_o = \pi r_s^2 d_{wx} \tag{2.4}$$

Where:

V_t = snow volume of cylindrical area around tree

V_s = volume of 1.5 m area around tree

r_s = radius of sphere

r_w = radius of well

d_{sc} = snow camera depth

V_w = volume of tree well

V_o = snow volume of open area under snow depth sensor

d_{wx} = weather station snow depth

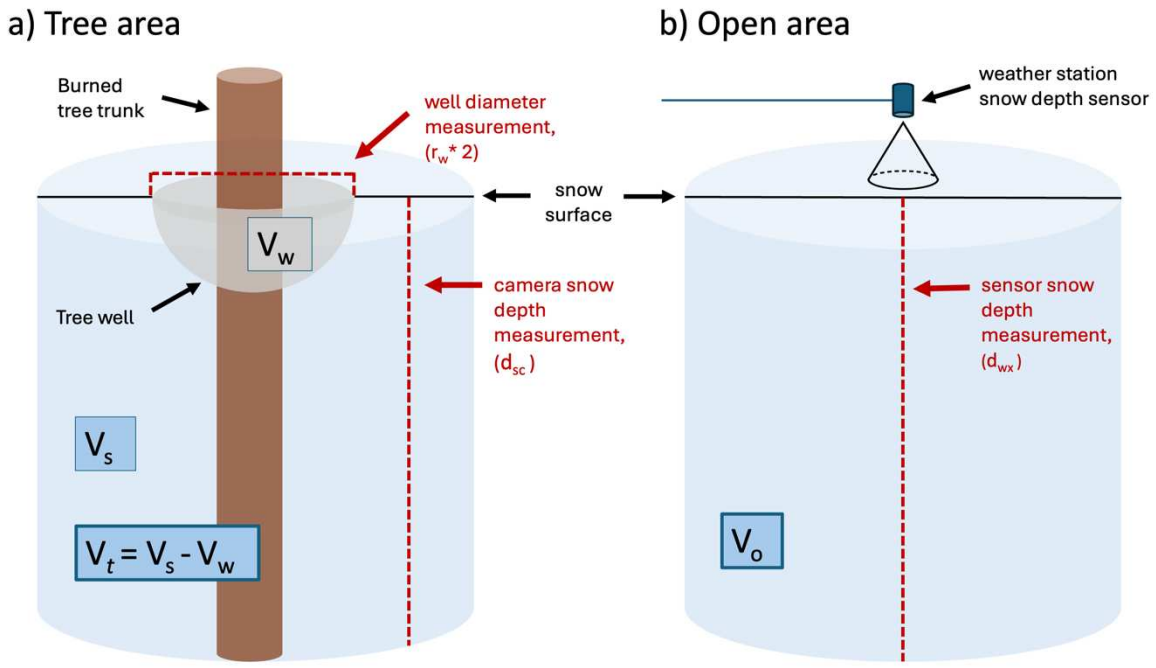

Figure 5. a) volume of snow calculated around tree, where V_w = volume of tree well, V_s = cylinder volume of snow around tree, and V_t = total volume of snow around tree, excluding the tree well and b) volume of snow calculated under weather station snow depth sensor where V_o = total volume of snow under sensor.

To understand the impacts of snow volume change on the total available snow water equivalent (SWE), the snow volume was converted to SWE using estimated snow density data from the Joe Wright (PSZ) and Hourglass Lake (TSZ) SNOTEL sites. The mean daily snow

depth and SWE data were converted to snow density time series; then the snow density values were used in combination with the site-specific daily snow depth to estimate SWE for burned sites. This snow density data was then used to convert the previously calculated snow volume for open and tree areas to SWE, using the following formulas:

$$i) \quad SWE_t = V_t * \rho_s \tag{2.5}$$

$$ii) \quad SWE_s = V_s * \rho_s \tag{2.6}$$

Where:

SWE_t = snow water equivalent in tree area

V_t = snow volume of cylindrical area around tree

SWE_s = snow water equivalent in open area

V_s = volume of 1.5 m area around tree

ρ_s = snow density

The mean absolute differences between tree and open areas snow volume and SWE were calculated for all four trees per site. The mean volume melt rate for tree and open areas were also calculated by computing the rate of volume change by day, then taking the mean of all days during the peak ablation period. These values quantified the rate of melt per day next to trees compared to in an open area.

3. RESULTS

3.1 Tree Surface Temperature

Before determining how burning affected tree temperatures, I first wanted to quantify the range of variability between replicate sensors, each measuring the same burn condition/aspect. Replicates of sensors for each burn condition and aspect had similar temperatures (Figure 6), with mean absolute differences < 0.8 °C on north aspects and ≤ 2.0 °C on south aspects (Figure 7), with standard deviations < 0.9 °C on north aspects and < 1.4 °C on south aspects (Table A1). The differences between DB and GB replicate sensors, by aspect, for both snow zones were within this same small range (0.6–1.6 °C, Figure 7). When the mean of the individual replicate DB and GB sensors were compared on the same aspect, the differences were still within this same range for both snow zones (1.1 and 3.0 °C during the day and 0.2 and 0.8 °C at night, Figure 8), indicating that, contrary to hypothesis 1.2.1 a., the differences in temperature between DB and GB trees are not clearly distinguishable from the variability between replicate sensors. The sensors have a stated average uncertainty of 0.04% relative to the temperature reading that increases with extreme cold and warm temperatures, meaning that a data value of 20 °C would have less than hundredth of a degree of uncertainty. My findings, while not statistically confirmed, do show that burned trees are warmer, on average, than live trees, which is consistent with hypothesis 1.2.1 b. Over the full snow season, burned trees were warmer during the day and cooler at night, which a mean absolute difference of 5.2 °C (GB) and 7.3 °C (DB) during the day and 1.8 °C (GB) and 2.6 °C (DB) at night in the PSZ (Figure 8, 9). In the TSZ the pattern remained the same, with warmer burned tree surface temperatures during the day and cooler at night compared to live trees. The mean absolute differences were greater at night (3.7 °C (DB)

and 4.7 °C (GB)) and not as high as in the PSZ during the day (2.9 °C (GB) and 5.7 °C (DB)) (Figure 8, 9). These comparisons by snow zone and day and night used the mean of all duplicate DB, GB and live sensors.

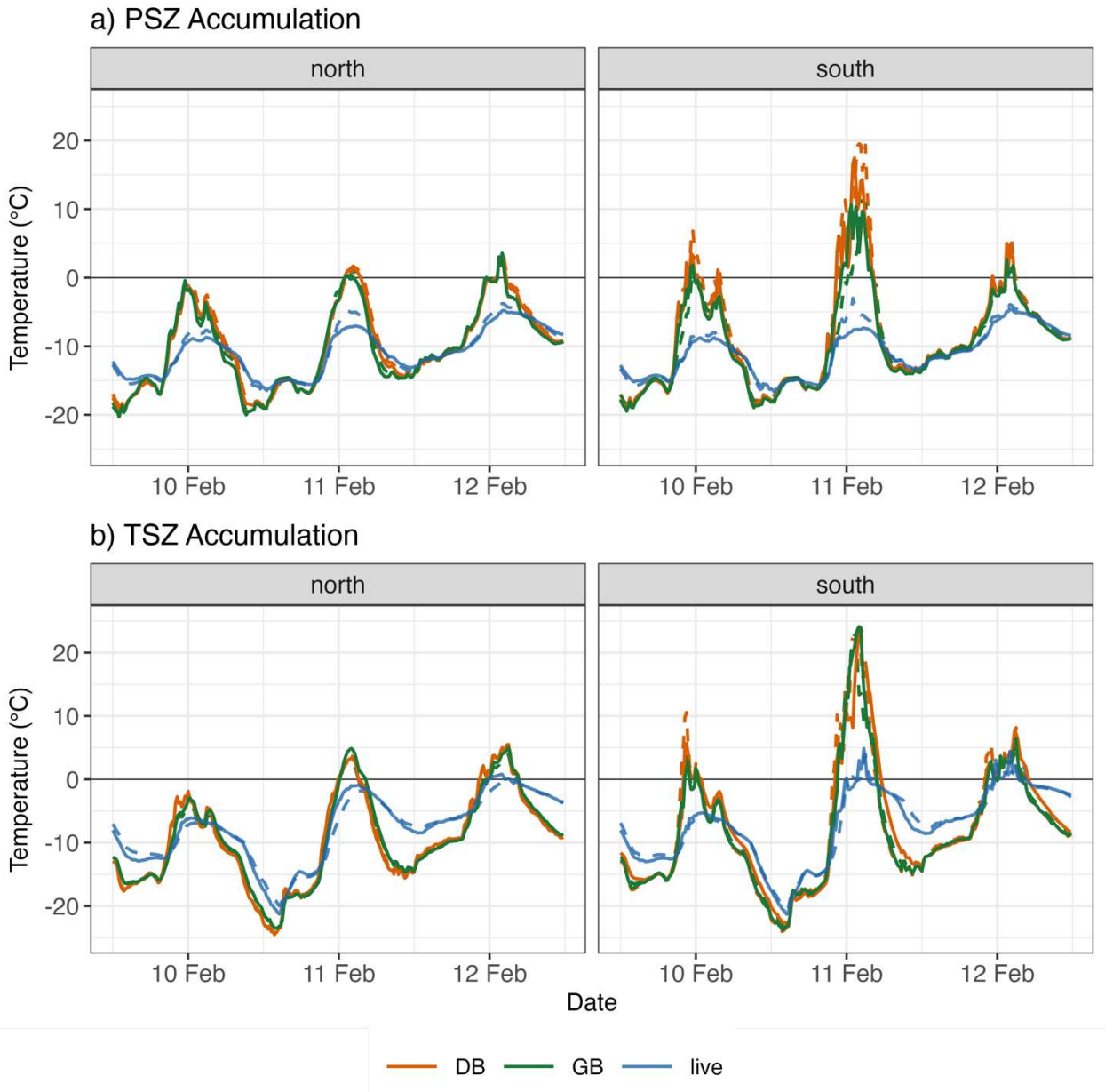

Figure 6. Individual sensor temperature comparison by condition (colors) and aspect in the a) persistent snow zone (PSZ) and b) transitional snow zone (TSZ). Tree 1 is represented by dashed lines and tree 2 is represented by solid lines. This is a three-day snapshot of time during the accumulation period from 10 February–12 February 2024.

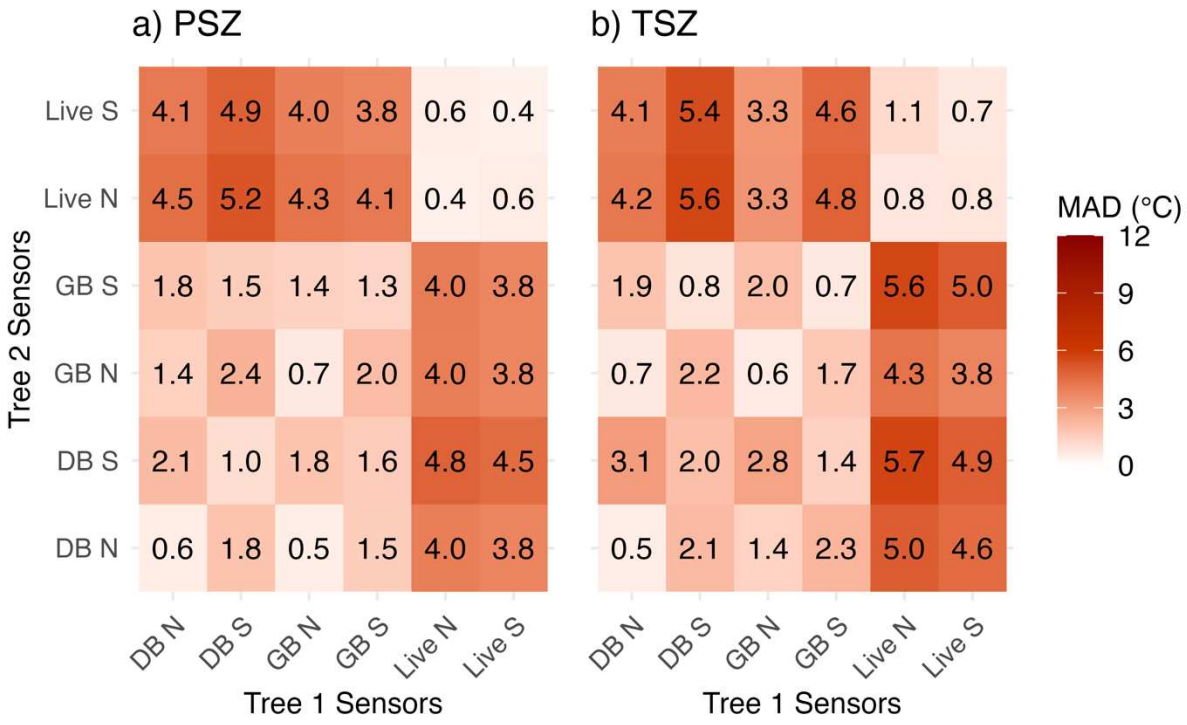

Figure 7. Temperature matrix comparing the mean absolute temperature differences (°C) (listed inside matrix) of replicate dead-burn (DB), green-burn (GB) and live sensors by burn condition and north (N) and south (S) aspect for the a) persistent snow zone (PSZ) and b) transitional snow zone (TSZ) from 2 February 2024–the snow-free date of each burned snow zone.

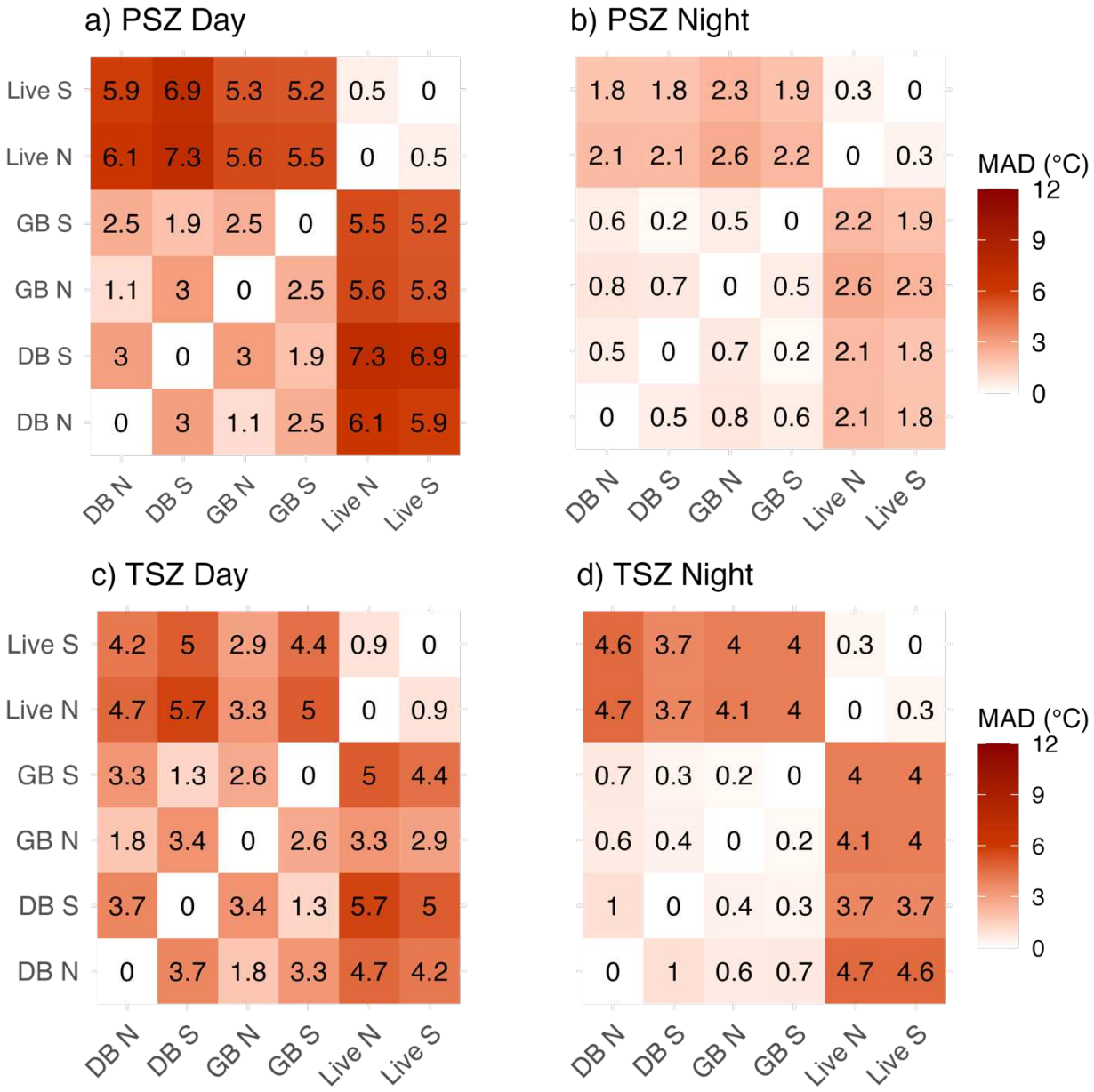

Figure 8. Temperature matrix comparing the mean absolute temperature differences (°C) (listed inside matrix) of mean dead-burn (DB), green-burn (GB) and live north (N) and south (S) sensors for the a) persistent snow zone (PSZ) and b) transitional snow zone (TSZ) from 2 February 2024 – the snow-free date of each burned snow zone.

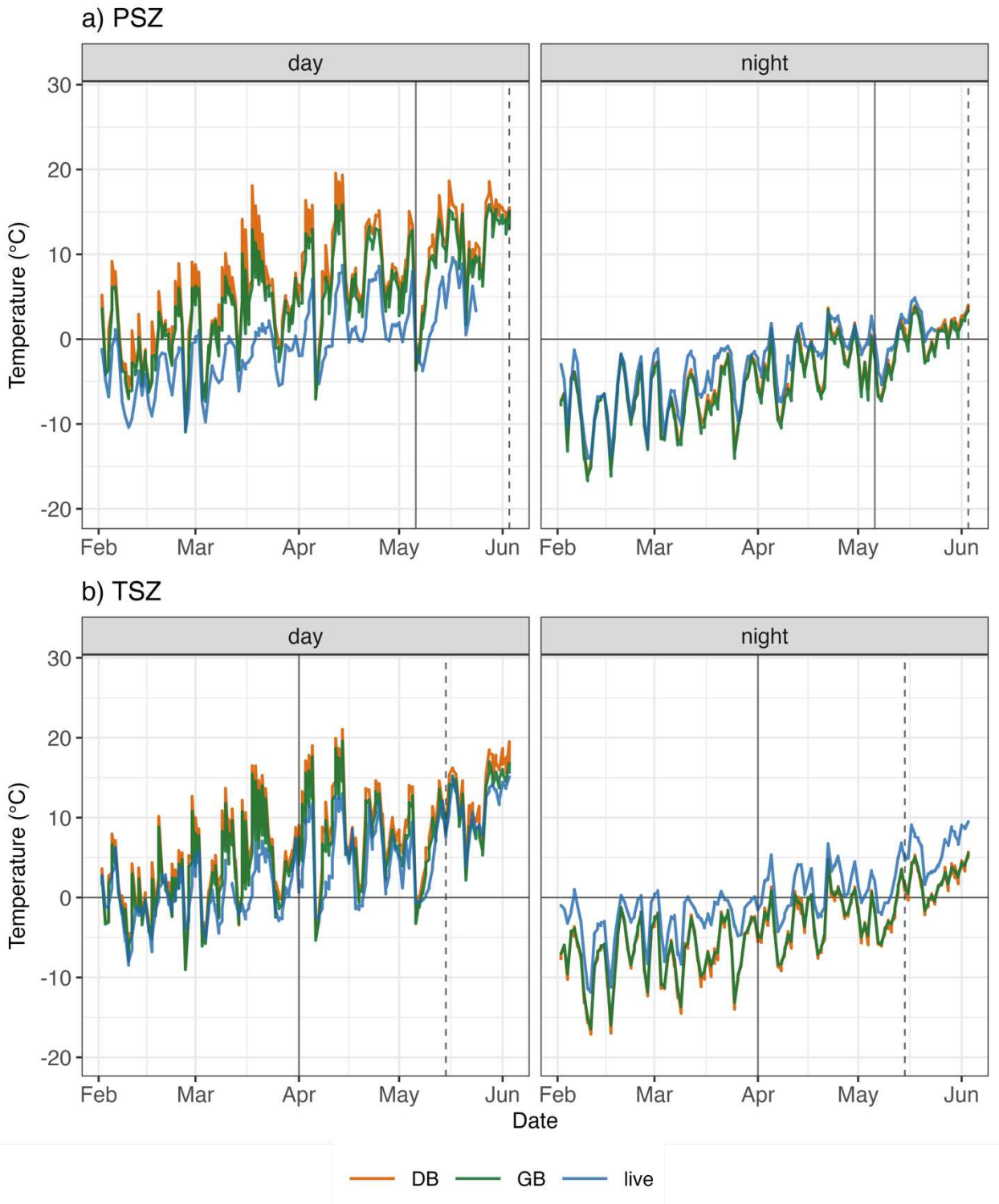

Figure 9. Daily mean tree surface temperature by burn condition for day and night groups in the a) persistent snow zone (PSZ) and b) transitional snow zone (TSZ) from 2 February 2024 – the snow-free date of each burned snow zone. The solid and dashed vertical line represents the beginning of ablation and snow-free date for each respective snow zone's burned site.

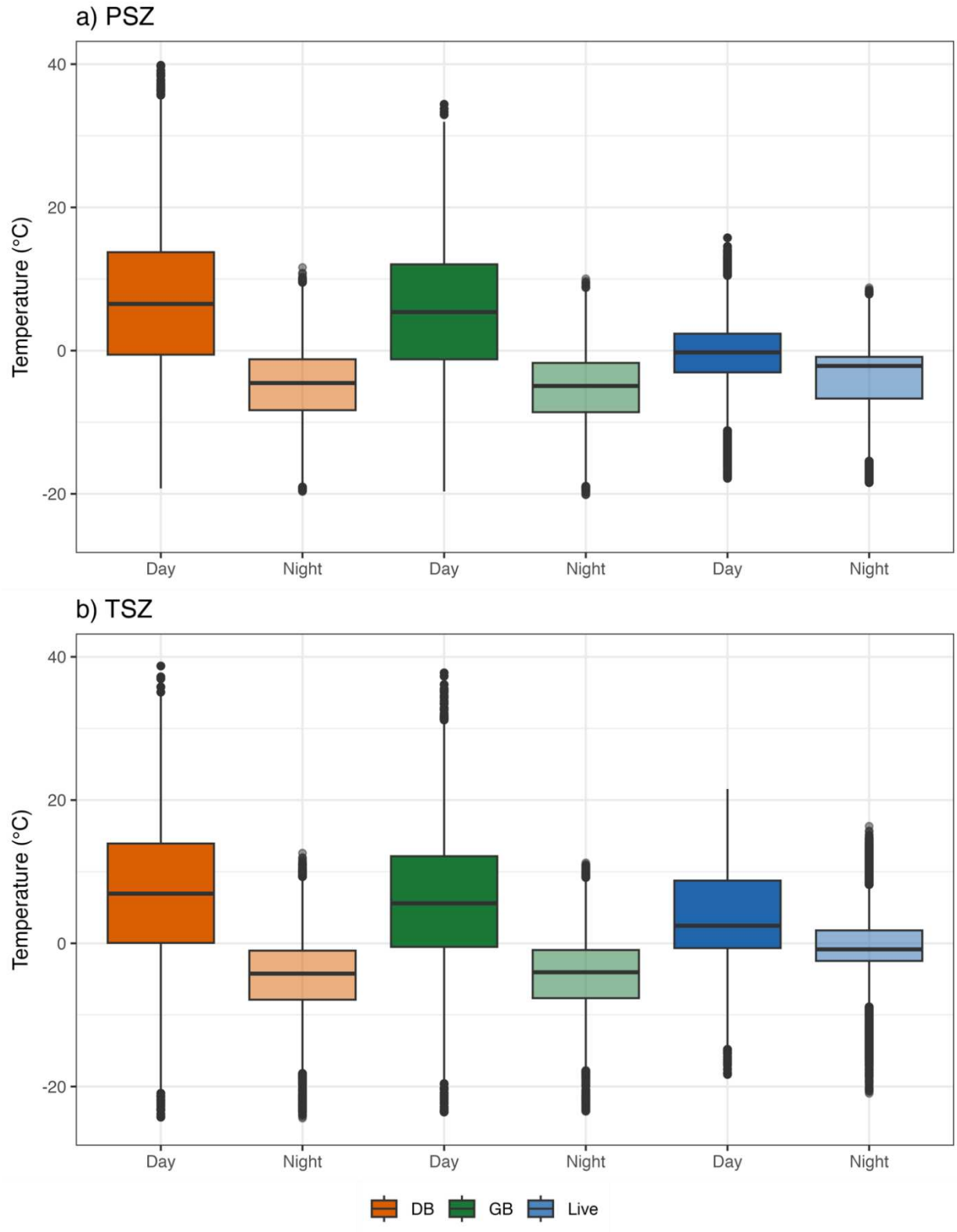

Figure 10. Boxplot of day and night temperature values by burn condition in a) persistent snow zone (PSZ) and b) transitional snow zone (TSZ) from 2 February 2024 – the snow-free date of each burned snow zone.

Comparing MAD of temperatures by aspect, the GB and DB trees had warmer daytime temperatures on south aspects compared to north aspects (range of 2.5–3.7 °C) for all DB and GB trees in both the PSZ and TSZ (Figure 8, 11), but the differences by aspect at night were minimal (range of 0.5–1 °C). Live trees had limited differences in temperature by aspect during both day (range of 0.5–0.9 °C) and night (0.3 °C) for both the PSZ and TSZ. The burned trees had large differences between day and night temperatures for all burn conditions on both north and south aspects (range of 10.3–11.5 °C and 10.2–11.6 °C for DB and GB trees in both snow zones, respectively; Figure 9, 10, 12). Live trees had lower temperature variations with an MAD range of 2.8–4.3 °C between day and night values for both snow zones. This difference of both DB and GB trees day and night temperatures was the largest temperature variation noted of all the comparisons (Figure 9, 10, 12).

The day and night temperature data were also separated to assess whether the temperature variations were different during the entire accumulation and peak ablation periods. This analysis showed similar patterns between day and night tree surface temperatures and between burn conditions. The main difference was that average daytime temperatures were higher and average night temperatures stayed near freezing for all burned conditions (Figure A1).

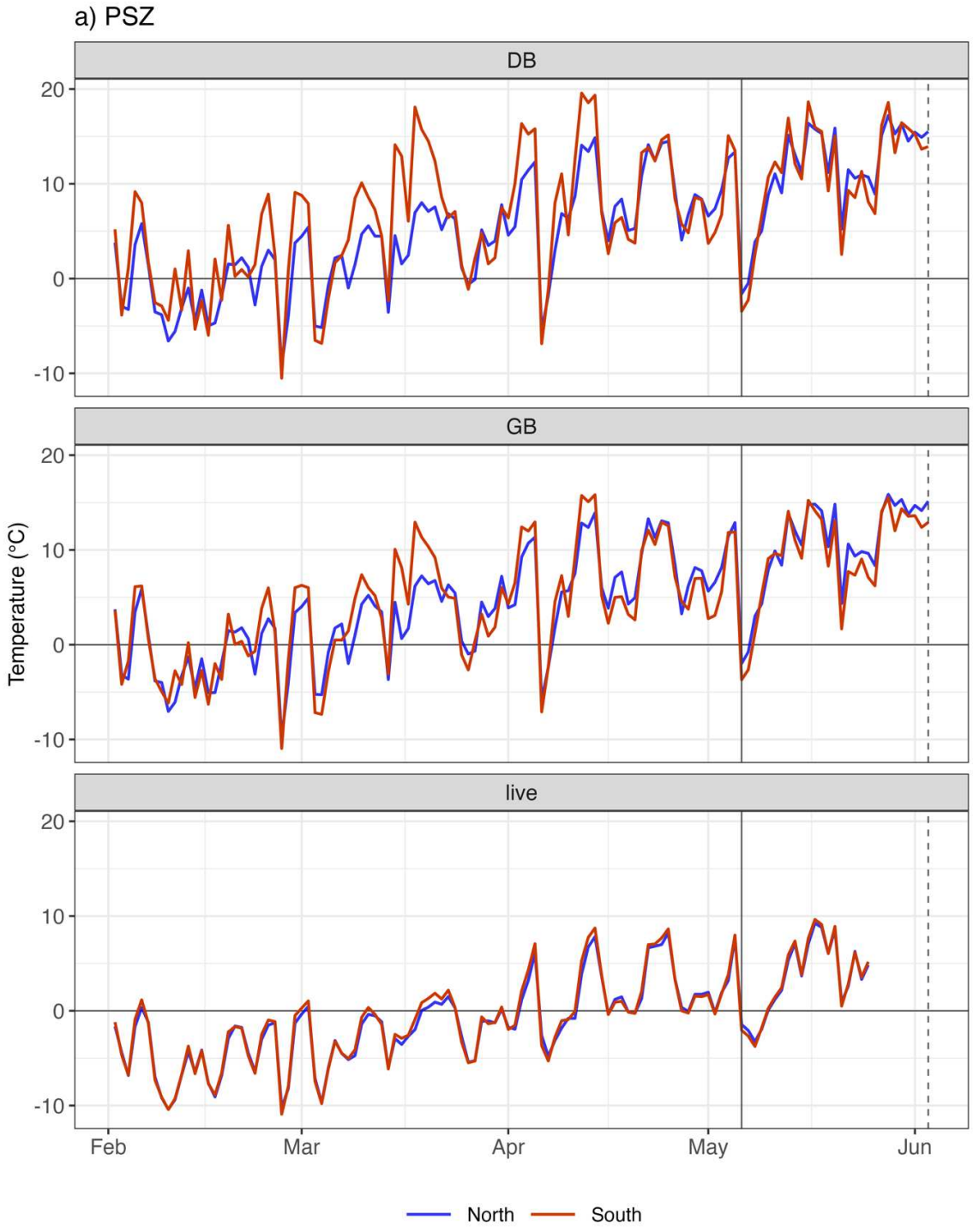

Figure 11. Mean daytime tree surface temperature colored by aspect for all dead-burn (DB), green-burn (GB) and live trees from 2 February 2024–the snow-free date of each burned site in the a) persistent snow zone (PSZ) and b) transitional snow zone (TSZ). The solid vertical line represents the beginning of ablation, and the dashed vertical line represents the snow-free date for each snow zone. Gap in PSZ live data was due to a data logger issue in which data was lost.

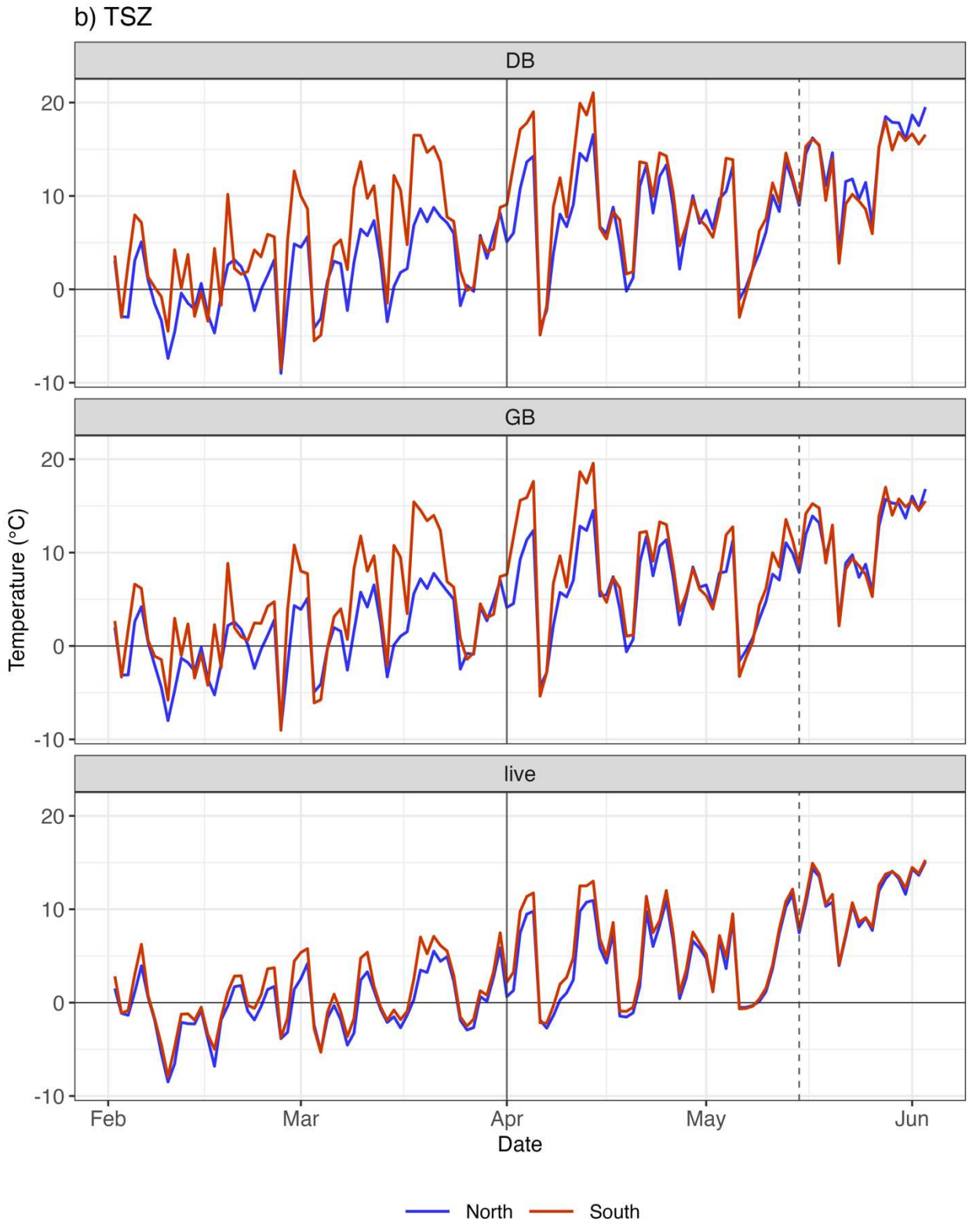

Figure 11. Continued...

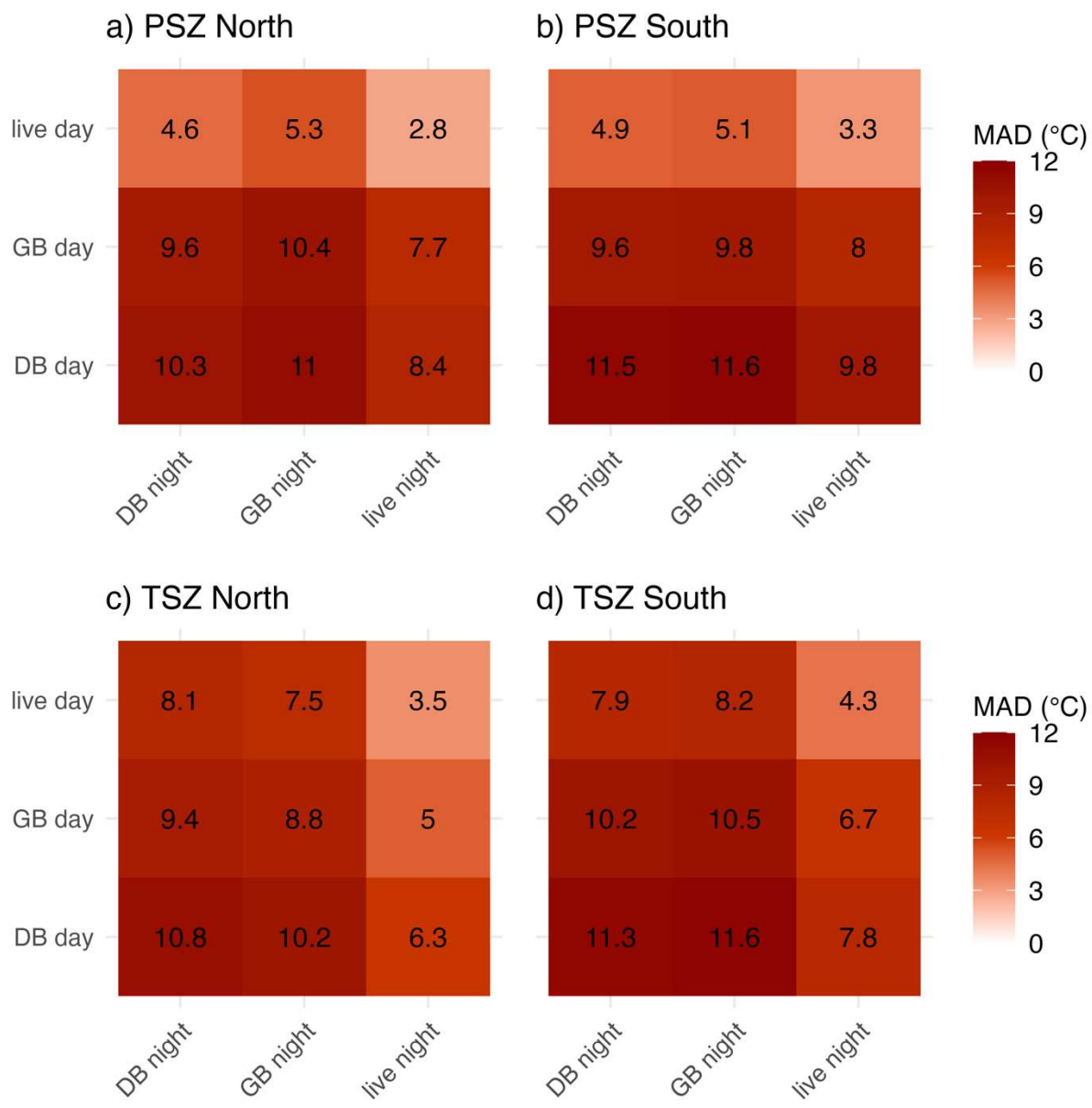

Figure 12. Temperature matrix comparing the mean absolute differences (°C) (listed inside matrix) of mean DB, GB and day and night temperatures for the a) persistent snow zone (PSZ) north sensors, b) PSZ south sensors, c) transitional snow zone (TSZ) north sensors and d) TSZ south sensors from 2 February 2024 – the snow-free date of each burned site.

3.2 Well Development

The study's objective for the well development analysis was to determine when tree wells developed around burned trees, how their size changed over time, and what factors affected the development of wells. Hypothesis 1.2.2 stated that the extent of well development would relate to both tree size (a) and tree temperature (b).

Snow camera data showed that tree wells occasionally formed during the accumulation season, but the pattern of development was sporadic (Figure 13). The wells would develop temporarily and then get refilled with new snow. In contrast, during peak ablation, when daytime air and tree surface temperatures were usually above freezing, and SWE and snow depths were consistently decreasing, wells developed and continued to increase in diameter until there was no longer snow surrounding the trees observed in both snow zones (Figure 13). The snow-free dates of the entire area observed from trail camera imagery for the PSZ and TSZ burned sites were 25 days apart, 15 May and 3 June, respectively. For context, the TSZ unburned site's snow-free date was 17 May, two days later than the burned site, while the PSZ's unburned site's snow-free date (from weather station due to data loss at snow camera) was 8 days later than the burned site, on 11 June 2024 (Figure 13). The snow-free dates of the tree wells analyzed below are different than the snow-free dates of the entire trail camera image, as they represent the point at which there was no longer consecutive snow around the individual trees observed.

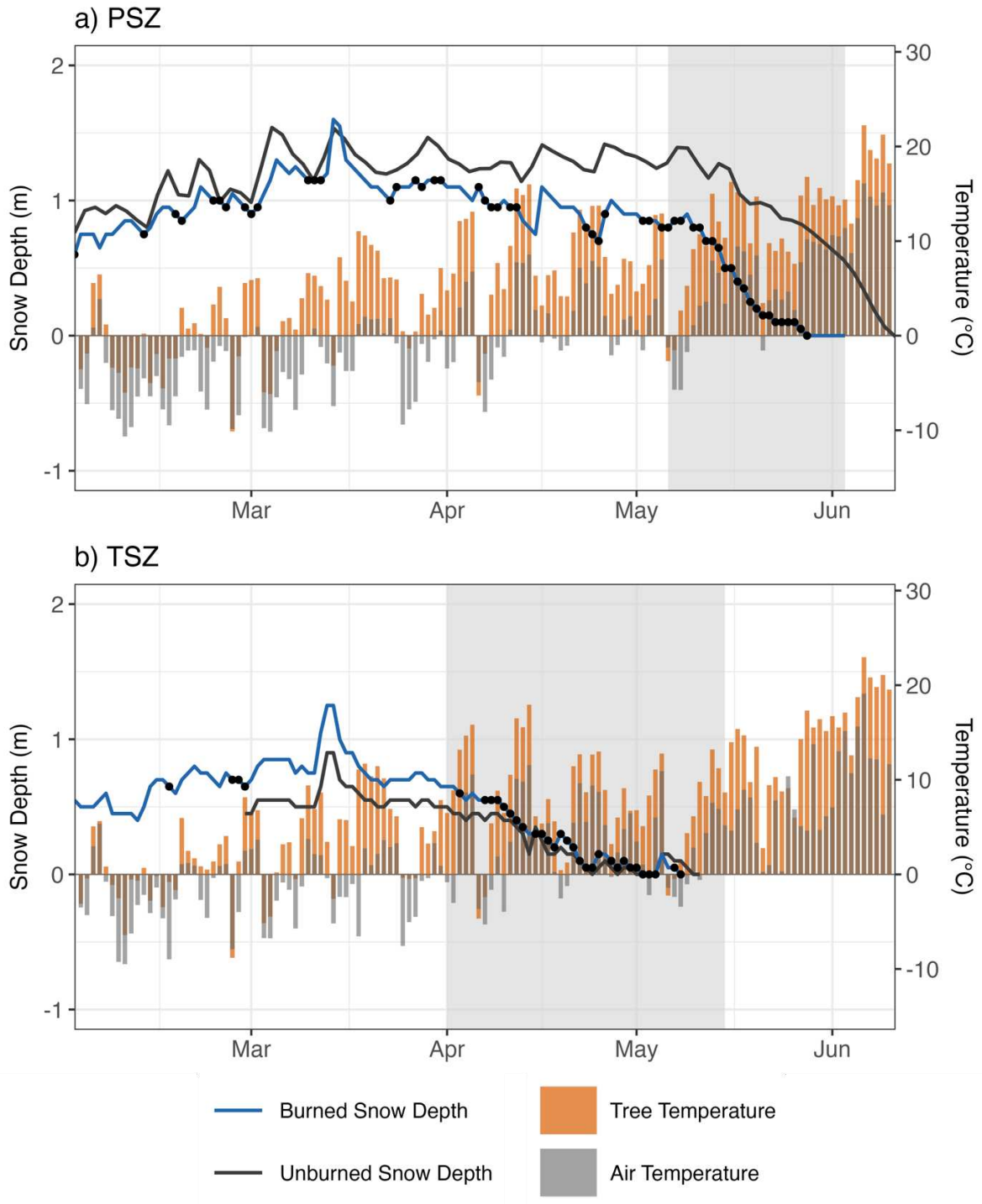

Figure 13. Maximum daily snow depth (m) from snow cameras and weather station data, mean daytime tree temperature (°C) of dead-burn and green-burn trees, mean daytime air temperature (°C) from weather station data, and dates that tree wells were present (black dots) in snow camera data for burned sites in the a) persistent snow zone (PSZ) and b) transitional snow zone (TSZ), from 2 February–15 June 2024 (PSZ unburned snow-free date). The grey rectangle in the background represents the peak ablation period for each respective snow zone.

Consistent with hypothesis 1.2.2 a., the manual tree well surveys showed that well diameters were positively correlated with tree diameter in both snow zones (R^2= 0.85 in PSZ, R^2= 0.71 in TSZ, p-value < 0.5 for both PSZ and TSZ) (Figure 14).

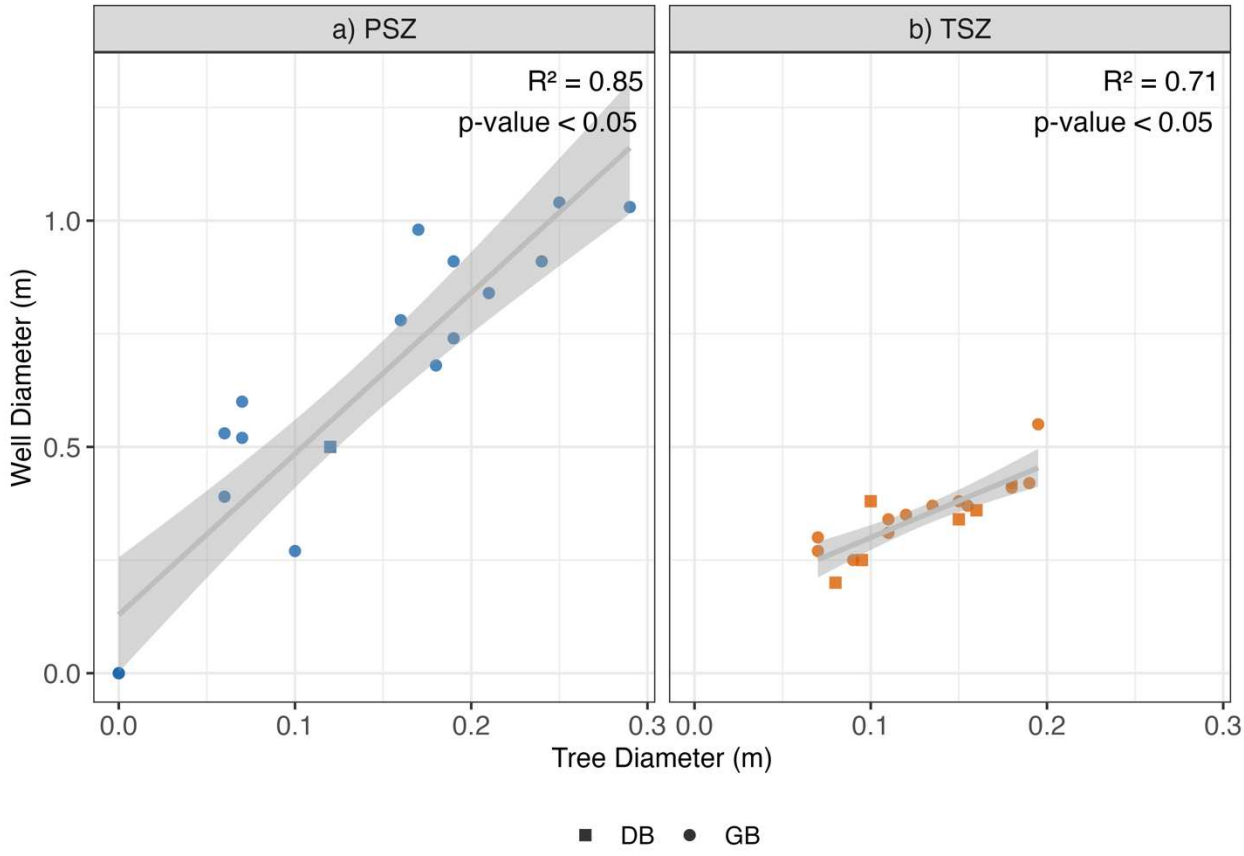

Figure 14. Tree diameter and well diameter (m) correlation scatterplots, with data taken from manual tree well surveys on a) 3 May 2024 for the persistent snow zone (PSZ) and b) 12 April 2024 for the transitional snow zone (TSZ). The shape of dots denotes burn condition, with squares representing dead-burn (DB) trees and circles representing green-burn (GB) trees.

My results also confirmed hypothesis 1.2.2 b. – Well diameters did increase with greater cumulative tree surface temperature during peak ablation. During accumulation, well diameter was not significantly correlated with cumulative tree surface temperature (mean $R^2 < 0.40$; mean p-value ≥ 0.05) in both snow zones (Figure 15, Table 3). In contrast, during peak ablation, cumulative daytime tree surface temperature was strongly correlated with an increase in well diameters in both snow zones, with a mean $R^2 = 0.86$ in PSZ and $R^2 = 0.77$ in TSZ and p-values < 0.05 in both zones (Figure 16, Table 3).

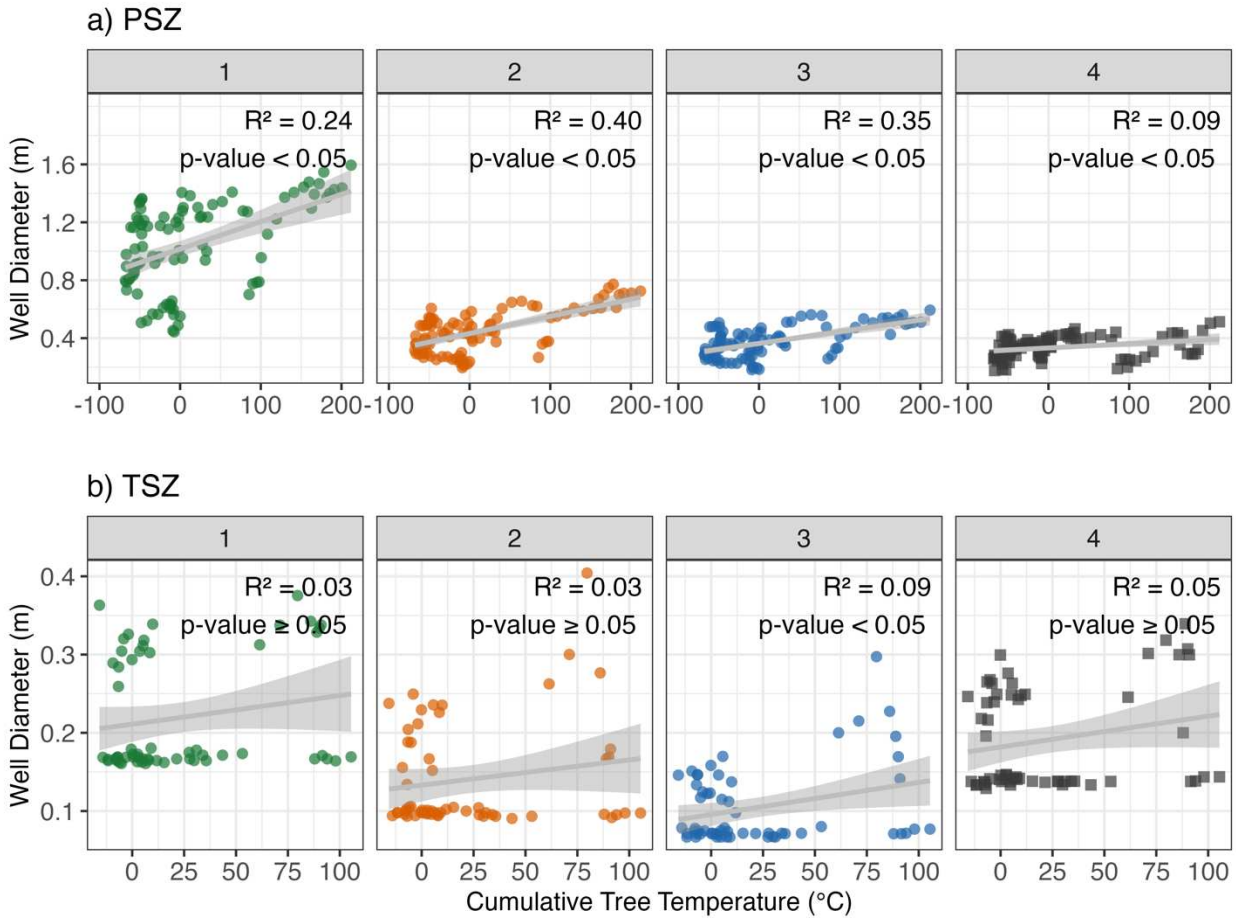

Figure 15. Well diameter (m) vs. cumulative tree surface temperatures (°C) during accumulation for four trees (colored by tree) within the site area of a) persistent snow zone (PSZ) and b) transitional snow zone (TSZ). The shape of dots denotes burn condition, with squares representing dead-burn (DB) trees and circles representing green-burn (GB) trees.

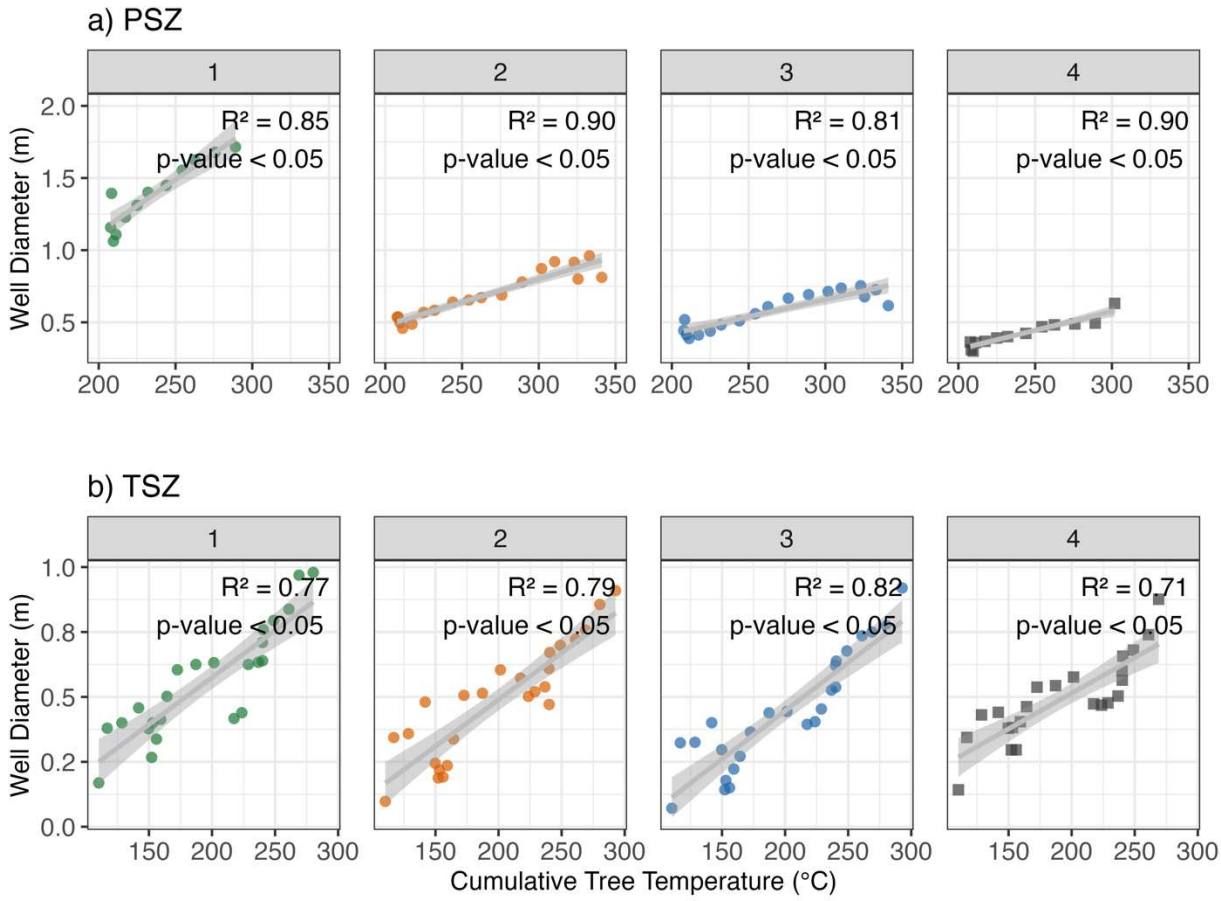

Figure 16. Well diameter (m) vs. cumulative tree surface temperatures (°C) during ablation for four trees (colored by tree) within the site area of a) persistent snow zone (PSZ) and b) transitional snow zone (TSZ). The shape of dots denotes burn condition, with squares representing dead-burn (DB) trees and circles representing green-burn (GB) trees.

Table 3. Pearson's correlation test results of well diameter and cumulative tree surface temperature (°C) during accumulation and peak ablation for four trees within the site area, separated by persistent (PSZ) and transitional (TSZ) snow zones. The values highlighted in blue are the R^2 results with a strong correlation.

Zone	Tree ID	Burn Condition	R^2	P-value	R^2	P-value
			Accumulation		Peak Ablation	
PSZ	1	GB	0.24	0.00	0.85	0.00
	2	GB	0.40	0.00	0.90	0.00
	3	GB	0.35	0.00	0.81	0.00
	4	DB	0.09	0.00	0.90	0.00
TSZ	1	GB	0.03	0.17	0.77	0.00
	2	GB	0.03	0.20	0.79	0.00
	3	GB	0.09	0.02	0.82	0.00
	4	DB	0.05	0.10	0.71	0.00

3.3 Melt Rate Comparison

The final objective of this study was to evaluate the differences of melt rates around trees compared to open areas. Hypothesis 1.2.3 a. stated that the increased tree surface temperature of burned trees would increase longwave radiation emitted by trees, leading to greater melt rates around burned trees relative to open areas. Results are consistent with this hypothesis, although I did not run statistical tests to confirm due to a small sample size (4 burned trees, 1 open area per snow zone). Because of variability in tree diameters (mean range of ± 0.32 m in the PSZ and ± 0.12 m in the TSZ) (Table 2), the melt rate findings are separated by tree in the tables but averaged for the results summary below. In the PSZ, the areas around trees had 18% lower snow volume on average compared to the open area during the accumulation and beginning of ablation season. This pattern continued into the peak ablation period, but the difference was larger, with tree areas having on average 39% lower snow volume than the open area (Figure 17, Table 4). In the TSZ, the tree and open areas daily mean snow volumes were similar (5% difference) during accumulation and the beginning of ablation but showed a marked difference during the peak

ablation period, when the tree areas had an average of 37% less snow compared to the open area (Figure 17, Table 4).

Overall, the snow around trees melted 69% faster during peak ablation and disappeared 8 days earlier than in the open area for the PSZ. This was also true in the TSZ, where snow melted 56% faster next to trees and disappeared 4–19 days earlier (range of all 4 trees) than in the open area (Figure 17, Table 4 & 5). In the PSZ, tree 1 had a diameter that was 0.26–0.36 m larger than all other trees, which led to substantially greater average difference in melt rates around this tree compared to the open area (Table 4). The patterns of volume change were similar for all burned trees, whether DB or GB (Figure 17, Table 4). When the snow volume melt rates were converted to SWE, the data showed the same pattern as snow volume changes; areas next to trees had decreased SWE compared to open regions during ablation (Figure B1, Table B1).

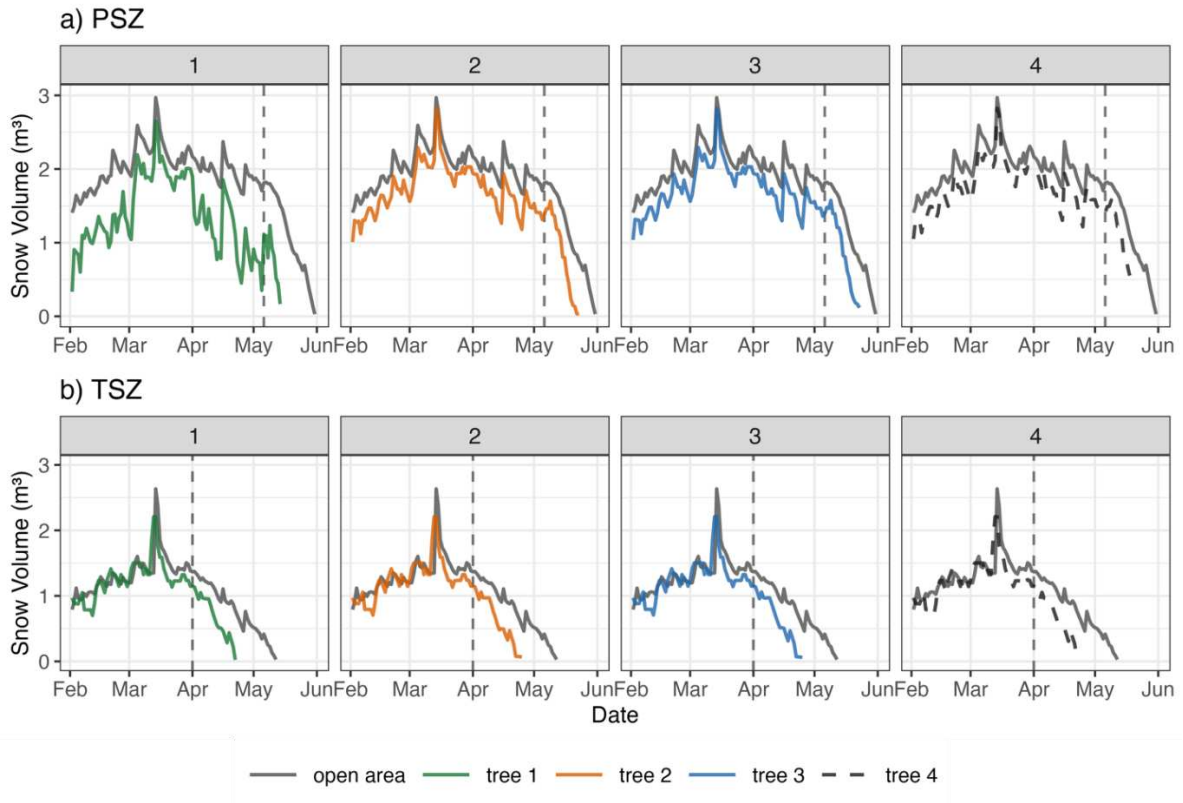

Figure 17. Snow volume time series for open and tree areas for the entire period of observation. The vertical dashed line represents the beginning of peak ablation period. Note that tree 4 is a dashed black line because it is a dead-burn (DB) tree, while trees 1–3 are green-burn (GB) in both plots a) persistent snow zone (PSZ) and b) transitional snow zone (TSZ). The lines that do not extend to zero had limited data due to the angle of the snow camera, so data are missing for the last part of the melt period.

Table 4. Mean percent difference between open and tree area snow volume (m^3) in the persistent (PSZ) and transitional (TSZ) snow zones during accumulation and ablation for all four observed trees per zone. The mean melt rate percent difference is also listed for the ablation season.

Zone	Tree ID	Burn Condition	Mean Volume % Difference Accumulation	Mean Volume % Difference Peak Ablation
PSZ	1	GB	31	38
	2	GB	15	37
	3	GB	14	37
	4	DB	14	36
TSZ	1	GB	5	54
	2	GB	5	39
	3	GB	5	36
	4	DB	5	26

Table 5. Ablation start and end dates by tree and open area for the persistent (PSZ) and transitional (TSZ) snow zones trail camera and weather station data. Asterisk (*) indicated trees where the trail camera's angle was too high to see the entire period of melt, so the date ranges do not represent the entire melt out period around the respective trees, but instead the latest date of observation. The open regions snow-free dates are when the snow depth camera sensors dropped to zero. The mean melt rate % difference was calculated during the peak ablation period.

Zone	Peak Ablation Start Date	Tree ID	Snow-free Date		Total days of peak ablation, *n*		Mean Melt Rate % Difference
			Tree Area	Open Area	Tree Area	Open Area	
PSZ	6 May	1	19 May *	31 May	13*	25	209*
		2	23 May		24		27
		3	23 May		23		20
		4	18 May *		12*		20*
TSZ	1 April	1	24 April	12 May	24	42	90
		2	9 May		39		31
		3	9 May		39		32
		4	23 April		23		81

4. DISCUSSION

This study compares tree surface temperatures, tree well development, and snow melt rates, in burned and live forests in the persistent and transitional snow zones of the Cache la Poudre River basin. I quantified how burning affected tree temperatures, tree well development and snowmelt rates to provide insights into how burned trees directly impact the total snow energy budget of a wildfire-impacted mountain ecosystem.

4.1 Snow Energy Balance

4.1.1 Tree Temperature

The results of this study highlight how burned trees can be a substantial source of energy to the snowpack post-fire. Their lack of canopy means that burned trees receive substantially more incoming shortwave radiation than unburned trees (Reis et al., 2024). The darker charred surface of burned trees absorbed even more incoming shortwave radiation due to their decreased albedo (Gleason et al., 2013). The increased shortwave absorption, coupled with increased emissivity (Kashiwagi et al., 1987) and tree surface temperatures result in a total increase in longwave radiation of burned trees. Although I had hypothesized that the extremely charred DB trees would warm even more than the trees with less extensive char (GB), the results did not show substantial differences between these two burn categories when compared by mean absolute differences (Figure 8 & 9). The higher sun exposure on both DB and GB trees may have been the primary driver of tree warming, with the extent of char cover having much less impact on tree temperatures. For all condition and aspects compared, both DB and GB trees were

warmer than live trees during daytime hours (Figures 9, 10 & 11), which is in alignment with hypothesis 1.2.1 b.

To further explore the relationship between tree surface temperature and seasonal changes in air temperature and shortwave radiation, I compared mean daytime tree surface temperature to mean daytime air temperature throughout the entire period of observation (Figure 18). These comparisons show that during daytime hours of the colder winter months, the tree surface temperature, air temperature and net shortwave radiation are lower than during spring months, when the days are longer, shortwave radiation increases and the air temperature is warmer, on average. The patterns and strong R^2 values noted in Figure 18 helps explain the relationship between increased shortwave radiation and increased tree surface temperature on a seasonal basis.

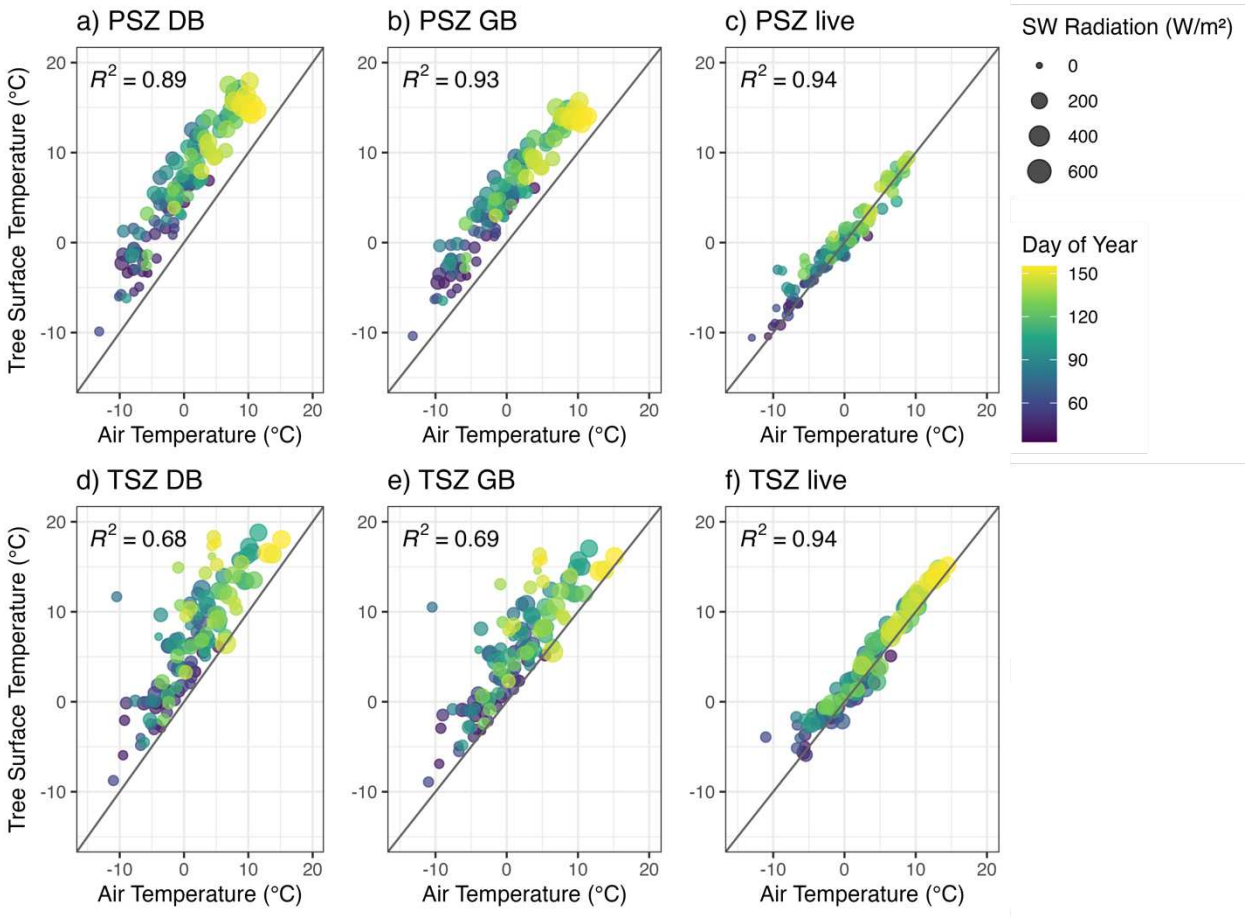

Figure 18. Daytime mean tree surface temperature compared to daytime mean air temperature for the a-c) persistent snow zone (PSZ) and d-f) transitional snow zone (TSZ) from 2 February–the snow-free dates of each zone. Sub-plots represent the dead-burn (DB), green-burn (GB) and live burn conditions. The mean daytime values are colored by day of year and sized based on the mean daytime net shortwave radiation values from each respective snow zone.

Prior research has found that southern, sunlit sides of live tree trunks and canopy warmed more during daytime hours, resulting in increased longwave radiation from southern aspects of trees (Pomeroy et al., 2009). In contrast, our results for live tree temperatures did not show substantial aspect-driven temperature differences (Figure 11). This is likely because the trees observed had continuous canopy cover on all aspects, shading the tree trunks from solar radiation. The burned trees are much more affected by aspect-dependent warming compared to live trees due to greater sun exposure (Figure 8 & 11). This is likely a product of winter months

in northern Colorado having short days and low sun angles, which creates a greater difference between north and south aspect daytime temperatures. The decreased north and south aspect temperature differences during the ablation period (Figure 11) is most likely caused by less of a sun angle difference in the spring months. More air mixing during longer daytime hours may also have reduced the aspect-driven temperature difference.

Canopy cover also contributed to differences in diurnal temperature patterns in burned trees compared to live trees. Live trees had lower daytime temperatures compared to burned trees (Figure 9 & 10) because of canopy shading (Wiscombe & Warren, 1980; Boon, 2009). Live tree night temperatures were higher than both DB and GB trees (Figure 9 & 10), likely because canopy cover in unburned forests insulates the live tree trunks. Live trees are also composed of approximately 35–50% water (compared to roughly 5% for burned trees), leading to a higher specific heat capacity and thermal inertia than burned trees, resulted in less heat loss to the surrounding atmosphere at night and decreased daytime temperatures (Kravka et al., 1999). The factors produce smaller diurnal temperature changes in unburned trees compared to burned trees, which had large day and night temperature differences (Figure 12).

4.1.2 Tree Wells

The effect of longwave energy emitted from a tree's canopy has been related to tree well development and increased snow melt rates around trees in unburned forests (Molotch et al, 2007; Molotch et al., 2016; Musselman & Pomeroy, 2017). Because unburned trees typically have more surface area in their canopies than in their trunks, the longwave influence of canopy cover is significantly higher than that of tree trunks in an unburned forest (Musselman & Pomeroy, 2017). In contrast, moderate to high severity burned forests lack any substantial canopy cover, so the longwave radiation that trees emit is primarily from the trunk. This study's

results showed that this energy emitted from the tree trunks results in snow melting directly around the burned trees, leading to the development of tree wells. As addressed in section 1.1, increased wind throughout burned forests also may lead to well development, although based on field observations, wind-shaped tree wells predominantly occurred during the accumulation period and were quickly refilled with new snow.

Manual well surveys showed that tree diameter influences well development, confirming hypothesis 1.2.2 a (Figure 14). Larger trees have larger well diameters, in part because the tree trunk takes up a significant portion of the middle of the diameter of a well when the well is measured from edge to edge on a horizontal plane, as was done in this study. However, the increased well development around larger trees are primarily because the radiation emitted by the larger tree trunk is coming from a larger surface area, leading to more energy for melting snow. Well diameter was found to be positively correlated with increased surface temperature during peak ablation, which is in agreement with hypothesis 1.2.2 b (Figure 16). Initially wells develop due to the proximity of snow and the warmer tree trunks, but as wells expand, the snow at the edge of the well extends farther away from the trunk. Musselman & Pomeroy (2017) found an exponential decline in potential melt energy from live tree trunks with distance from the trunk. This finding helps explain why the wells are deepest right next to the tree and shallower at the outer edges (Figure 4a & b).

4.2 Snow Melt Rates

Prior studies have already found that snow-free dates can be earlier post-fire due to changes in shortwave radiation (Wiscombe & Warren, 1980; Boon, 2009; Gleason et al., 2013; Gleason et al., 2019; McGrath et al., 2023), and this study shows that tree wells can advance snow-free dates around burned trees by 8–16 days compared to open regions. I hypothesized that

the longwave radiation emitted by burned trees would decrease snow volume directly around trees compared to open areas of a burned forest, and the results, while not statistically tested, did agree with this pattern (Figure 17, Table 4). The melt out directly around trees was increased by warmer tree surface temperatures creating faster melt around the trees. This bare ground's dark color after a fire decreases the snow albedo inside a well and further accelerates melt out directly next to trees. Figure 19 shows a time series of trail camera images, depicting the snowmelt patterns around trees post-wildfire. Initially the wells are small but the rate of well expansion increases rapidly as snow depths decrease and bare ground is exposed. Where a burned forest has a large number of standing trees, the increased melt rates around the trees likely has a very substantial influence on accelerating the snowmelt rates of a burned forest.

To gather a rough estimate of the extent of tree well's impact on a larger area, I analyzed drone imagery and of the TSZ burned site in ArcGIS Pro for a 35-m^2 region around the sensors and weather station locations, which had 233 standing burned trees (Figure 20). Using section 2.3.3. methodology, I applied well diameter and snow depth data to the 233 standing burned trees and the remainder of the open area to calculate snow volume around the trees and in the remaining open area of the 35-m^2 region (Figure 21). When the total tree snow volume was subtracted from the remaining open regions snow volume, there was a 27% total snow volume loss from the tree wells for the entire period of observation. While assumptions are made by applying one known tree's daily well diameter to all the trees, these rough calculations further suggest that there is a substantial amount of snow volume loss due to tree wells across a forested region. Therefore, considering the varied snow melt around trees compared to open regions of a burned forest is critical for better understanding snowmelt patterns post-wildfire.

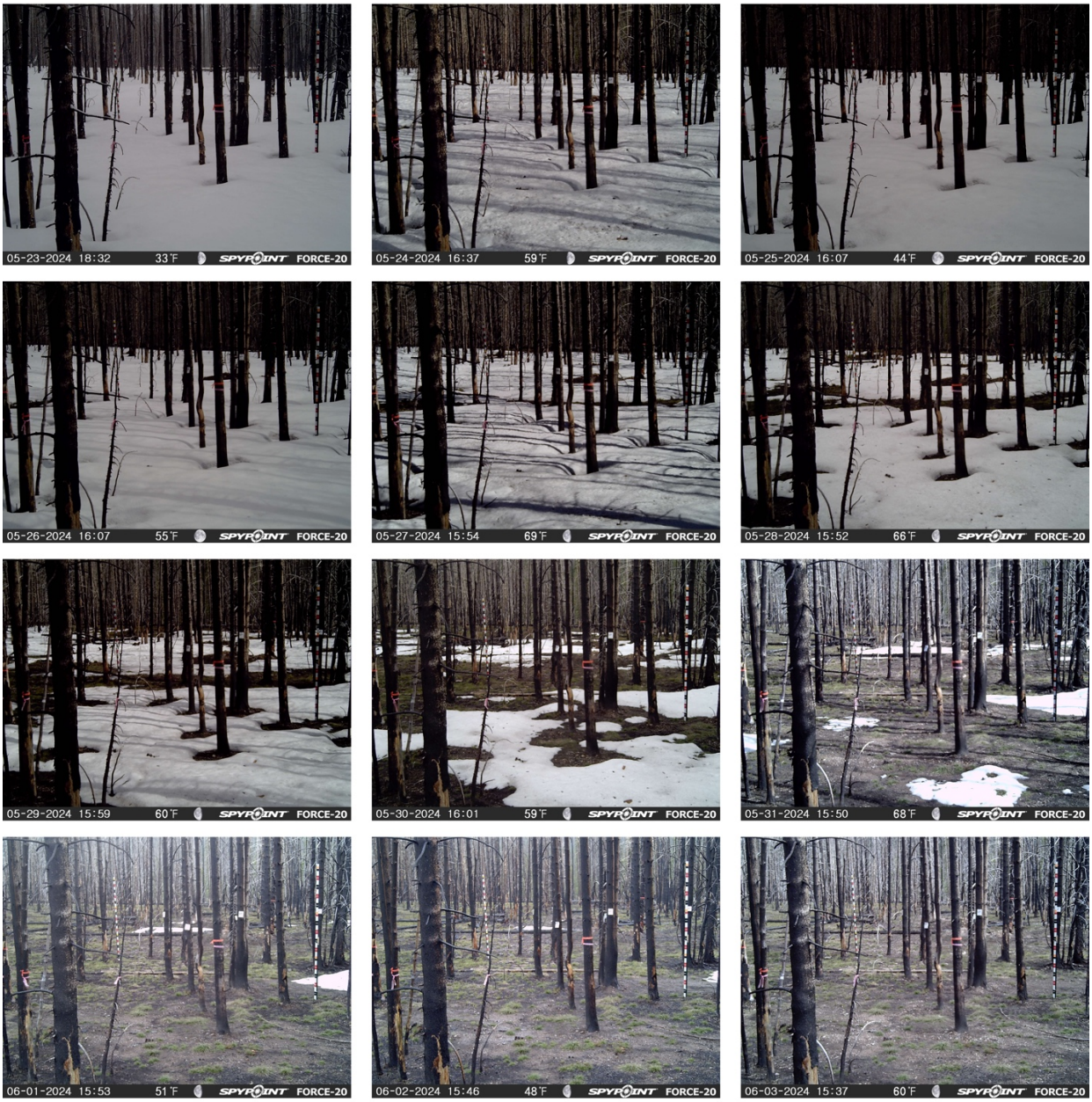

Figure 19. Persistent snow zone trail camera imagery from 23 May–3 June 2024, showing the well development and melt pattern around burned trees compared to open regions.

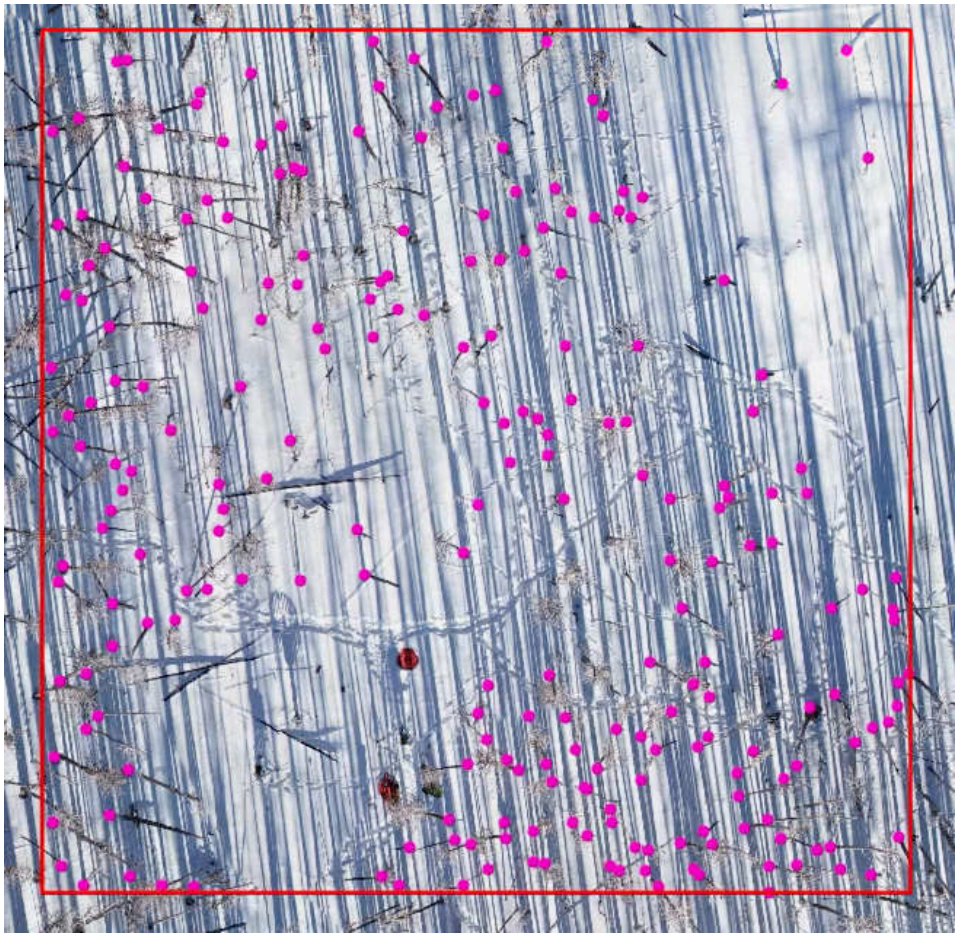

Figure 20. Drone imagery of the 35-m^2 area (red outline) in the transitional snow zone with the standing burned trees represented by pink dots.

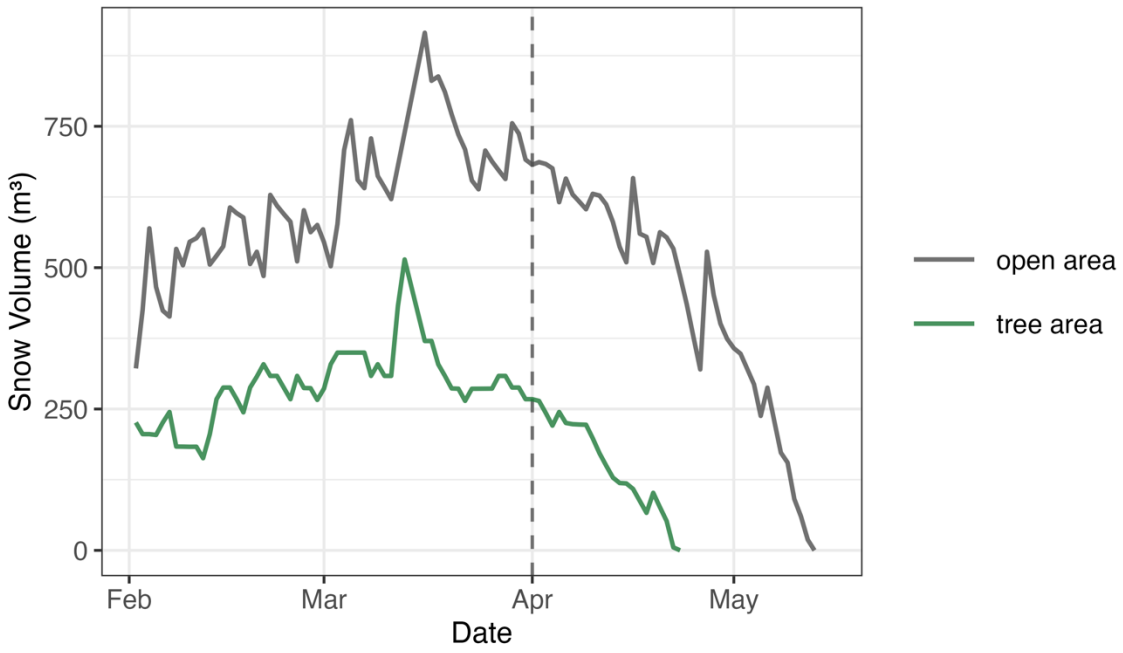

Figure 21. Snow volume time series for open and tree areas of a 35-m^2 area at the transitional snow zone's burned site from 2 February–the open regions snow-free date. The vertical dashed line represents the beginning of peak ablation. The tree area snow volume is the sum of all 233 trees and the open area snow volume is the remaining area's snow volume not impacted by tree wells.

In unburned, canopy-covered forests snow may persist longer in open regions compared to under the tree canopy because of both lower snow accumulation and higher longwave radiation from the forest canopy that melts snow directly next to trees (Hubbart et al., 2015; Molotch et al., 2016). In burned conditions, the earlier snow disappearance around trees is predominantly due to longwave radiation emitted by the warm tree trunks, since the minimal remaining branches do not effectively intercept snow or emit substantial radiation. Burned forests may also have increased sublimation compared to unburned forests because of higher wind speeds (Boon, 2009; Molotch et al., 2009, Reis et al., 2024). However, sublimation is not likely the dominant process creating tree wells. Wells primary developed during the peak ablation period, when tree temperatures were well above freezing (Figure 13). These warm temperatures were high enough to melt the snow surrounding the trees. During the accumulation

period, some wells appeared to develop during wind events, which might have been the initial stages of later tree surface temperature-driven well development, but more research is needed to assess this potential early-season driver of well development. To confirm that the tree wells are caused by melt, it would be helpful to have snow temperature measurements around the well to determine if the snow itself has reached 0°C as wells develop. More research into snow density distributions around tree wells, as well as the cumulative effect of increased snow melt around individual burned trees, would assist in explaining the patterns of melt rates in burned forests noted in this study.

Since the tree wells were measured in two different snow zones, the results give some insight into how the burned tree effect on snow may vary spatially. From the data showing tree well development dates and tree surface temperature, the snow-free date of tree areas was 23 April – 9 May 2024 in the TSZ, whereas tree areas in the PSZ were snow-free later (18 May–23 May) (Table 5). In the TSZ, the trees were snow-free 3–10 days earlier than the open area, whereas in the PSZ the trees were snow-free 8–13 days earlier than in the open area. However, the period that snow existed around trees during the ablation period was 2 days shorter (Table 5), and the snow melted 23% faster (average of all 4 trees per site) in the PSZ than in the TSZ (Figure 17, Table 5). Because the ablation period was later in the PSZ, daytime tree surface temperatures were 2.9 °C warmer, on average, than temperatures during the TSZ ablation period (Figure 13). The later timing of melt in the PSZ likely led to greater melt rates and greater advances in snow-free dates than in the TSZ. In the future, these findings could be combined with forest density data to further improve larger-scale analysis of differences in SWE and snow melt rates of wildfire-impacted forests.

4.3 Temporal and Spatial Context

These observations were made in the fourth winter/spring post-fire. Prior research has shown that the impacts of wildfire can last for decades (Gleason et al., 2019), and these impacts shift with the years. Decreased albedo due to char on snowpack is primarily found in years 1–3 post-fire years (Gleason et al., 2016). Deadfall increases after 3–5 years (Angers et al., 2011), and therefore decreased canopy becomes more of a driving factor for increased shortwave radiation, and the longwave radiation input from trees will decrease. If this research had been done year-one post-fire, there would have likely been more DB and GB trees left standing, significantly more char deposited around the tree trunk and on the snow surface, potentially leading to an even greater difference between burned and live tree's surface temperature and resulting well development. As more winters pass, there will likely be even fewer trees left standing and potentially even less char coverage on standing trees. Without standing trees, tree wells will no longer develop and accelerate melt rates.

These observations were gathered in the continental snowpack region of the Southern Rocky Mountains in Colorado – a region that typically has shallower snowpack, larger diurnal air temperature shifts, and significantly more solar radiation during winter months than the intermountain or maritime snowpack regions of the western US (Mock & Birkeland, 2020). The substantial amount of winter solar radiation and diurnal air temperature fluctuations help explain the trends noted between burned and live tree surface temperatures during the day and night hours. Regions with larger trees and/or increased tree density that have substantial mid-winter solar radiation will likely see a net increase in the longwave radiation contribution of trees to the total snow energy budget of a burned forest, potentially resulting in increased snow volume loss around trees and even earlier snow-free dates for wild-fire impacted forests. In wildfire-impacted

regions with less winter solar radiation, the difference between burned and live tree temperatures and resulting well development might be less important for the overall post-fire snow energy budget.

4.4 Project Limitations

4.4.1 Study Area

For consistency purposes, I attempted to find burned and unburned sites with similar aspects. Due to the burn pattern in both snow zones and site access constraints, the PSZ unburned site's aspect was southeast (~150°) while the PSZ burned site and TSZ burned and unburned sites aspect were northwest (~315°). However, because all these sites had low surface slopes (~ < 5°), it is unlikely that these aspect differences significantly altered the results. The site with the different aspect (unburned PSZ) also has tree canopy cover, which limits aspect-driven differences in radiation and snow processes.

The unburned TSZ site with tree temperature sensors and weather station had significantly lower snow depths than all other sites. This difference was largely topography-driven, and not a reflection of the relationship between burn pattern and snow persistence. The TSZ unburned site is located in a wide valley, with the northern end of the Mummy Mountains sitting directly southwest of the site. This site has high downslope winds that blow snow away from the snow stake, camera and snow depth sensor. For that reason, a secondary location's snowpack depth data was used for the unburned TSZ that was in a more protected area of unburned trees, near the TSZ burned site (Figure 13). This secondary location was closer to the TSZ burned site, and more accurately represented the large-scale conditions of an unburned forest, however it still had lower snow depths than the TSZ burned site for most of the winter

and spring. This was likely a product of the trail camera being located in a highly forested pocked where snow did not accumulate well compared to the open region of the TSZ burned site.

4.4.2 Well Development and Snow Volume Calculations

Due to a time constraint and lack of quality imagery of live trees, live tree well development was not analyzed. This meant that the melt rate comparisons could only be made around burned trees and in open regions of a burned forest. In the burned tree well measurements, the well volumes were not noticeably different around DB and GB trees, which is consistent with the similar temperatures between these two tree types. However, the camera imagery used for this part of the project only had one DB tree per site available to analyze for tree wells, and a greater sample size would be needed to definitively determine if there are any differences in well sizes between DB and GB trees.

This study primarily addresses snow volume instead of SWE because I did not have site-specific daily snow density data; therefore, a snow volume analysis at each site more accurately represented this project's study sites. I did, however, predict differences in SWE melt volume between treed and open areas based on the snow volume calculations (Table B1, Figure B1). The predicted snow density values used to calculate SWE melt volume were from two SNOTEL sites not directly next to my study areas, with different topography and orographic conditions. Consequently, the SWE melt volume comparisons are more of an estimate than a precise calculation.

5. CONCLUSION

Wildfires change snow processes by altering the snow accumulation and ablation rates and energy budget of a forest. A key, yet often overlooked, component of the post-fire energy budget is longwave emissions from burned trees. To address this, I quantified tree surface temperature differences between burned and live trees and the resulting snow volume and melt rates around burned trees compared to open regions. This allowed us to better understand the influence of burned trees on the total radiation budget of a post-fire, snow-covered forest. This research shows that burning impacts the amount of heat retained and emitted by burned trees. I found that burned trees' daytime temperatures were 2.9–7.3 °C warmer on average than unburned trees, with daytime temperatures of burned trees well above freezing for most of the snow season. Due to these high temperatures, tree wells developed around burned trees, and their size increased with greater cumulative tree surface temperature and with larger tree diameters. Because of the tree wells, snow volume around trees decreased 56–69% faster during the ablation season than in open regions. This led to snow melting 8–16 days earlier directly around burned trees compared to open areas. Since open areas already have accelerated melt rates compared to unburned forests, adding in the effect of burned trees further expands the differences in snow melt rates and snow-free dates between burned and unburned forests.

Future work could benefit from incorporating defined tree surface temperatures and emissivity of burned trees into radiation flux calculations, using the Stefan-Boltzman law, to more accurately quantify burned tree’s longwave radiation contribution to the total energy budget of a wild-fire impacted forest. This would, in turn, provide more context for snow melt rates in a burned forest compared to that of an unburned forest. These findings can be used to

improve snow energy budget models and predictions of snowmelt runoff and water availability in a wildfire-impacted mountain ecosystem. This information will provide critical improvements to water management throughout regions that are dependent on snow as a main water source.

REFERENCES

Adam, J. C., Hamlet, A. F., & Lettenmaier, D. P. (2009). Implications of global climate change for snowmelt hydrology in the twenty-first century. *Hydrological Processes*, *23*(7), 962–972. https://doi.org/10.1002/hyp.7201

Angers, V. A., Gauthier, S., Drapeau, P., Jayen, K., & Bergeron, Y. (2011). Tree mortality and snag dynamics in North American boreal tree species after a wildfire: a long-term study. *International Journal of Wildland Fire*, *20*(6), 751–763. https://doi.org/10.1071/WF10010

BAER (Burn Area Emergence Response) (2023). Soil Burn Severity Dataset for the CAMERON PEAK Fire occurring on the Arapaho & Roosevelt National Forests/Pawnee National Grasslands Forest. USDA Forest Service. https://burnseverity.cr.usgs.gov/baer/baer-imagery-support-data-download

Barnett, T. P., Adams, J. C., & Lettenmaier, D. P. (2005). Potential impacts of a warming climate on water availability in snow-dominated regions. *Nature*, *438*(7066), 303–309. https://doi.org/10.1038/nature04141

Barnett, T. P., Pierce, D. W., Hidalgo, H. G., Bonfils, C., Santer, B. D., Das, T., Bala, G., Wood, A. W., Nozawa, T., Mirin, A. A., Cayan, D. R., & Dettinger, M. D. (2008). Human-Induced Changes in the Hydrology of the Western United States. *Science (American Association for the Advancement of Science)*, *319*(5866), 1080–1083. https://doi.org/10.1126/science.1152538

Bode, E. T., Lawrence, R. L., Powell, S. L., Savage, S. L., & Trowbridge, A. M. (2018). Time-series approach for mapping mountain pine beetle infestation extent and severity in the U.S. Central Rocky Mountains. *Journal of Applied Remote Sensing*, *12*(4), 046030–046030. https://doi.org/10.1117/1.JRS.12.046030

Boon, S. (2009). Snow ablation energy balance in a dead forest stand. *Hydrological Processes*, *23*(18), 2600–2610. https://doi.org/10.1002/hyp.7246

Davis, R. E., Hardy, J. P., Ni, W., Woodcock, C., McKenzie, J. C., Jordan, R., & Li, X. (1997). Variation of snow cover ablation in the boreal forest: A sensitivity study on the effects of conifer canopy. *Journal of Geophysical Research, Washington, DC*, *102*(D24), 29389–29395. https://doi.org/10.1029/97JD01335

Gleason, K. E., McConnell, J. R., Arienzo, M. M., Chellman, N., & Calvin, W. M. (2019). Four-fold increase in solar forcing on snow in western U.S. burned forests since 1999. *Nature Communications*, *10*(1), 2026–2026. https://doi.org/10.1038/s41467-019-09935-y

Gleason, K. E., Nolin, A. W. (2016). Charred forests accelerate snow albedo decay: parameterizing the post-fire radiative forcing on snow for three years following fire. *Hydrological Processes, 30*(20), 3855–3870. https://doi.org/10.1002/grl.10897

Gleason, K. E., Nolin, A. W., & Roth, T. R. (2013). Charred forests increase snowmelt: Effects of burned woody debris and incoming solar radiation on snow ablation. *Geophysical Research Letters*, *40*(17), 4654–4661. https://doi.org/10.1002/grl.50896

Hammond, J.C., 2020, *Contiguous U.S. annual snow persistence and trends from 2001-2020*: U.S. Geological Survey data release. https://doi.org/10.5066/P9U7U5FP

Hardy, J. P., Albert, M. R., Albert, M., & Taylor, S. (1995). Snow-induced thermal variations around a single conifer tree. *Hydrological Processes*, *9*(8), 923–933. https://doi.org/10.1002/hyp.3360090808

Hardy, J. P., Davis, R. E., Jordan, R., Li, X., Woodcock, C., Ni, W., & McKenzie, J. C. (1997). Snow ablation modeling at the stand scale in a boreal jack pine forest. *Journal of Geophysical Research. D. Atmospheres*, *102*(D24), 29–405. https://doi.org/10.1029/96JD03096

Hubbart, J. A., Link, T. E., & Gravelle, J. A. (2015). Forest Canopy Reduction and Snowpack Dynamics in a Northern Idaho Watershed of the Continental-Maritime Region, United States. *Forest Science*, *61*(5), 882–894. https://doi.org/10.5849/forsci.14-025

Kampf, S. K., McGrath, D., Sears, M. G., Fassnacht, S. R., Kiewiet, L., & Hammond, J. C. (2022). Increasing wildfire impacts on snowpack in the western U.S. *Proceedings of the National Academy of Sciences - PNAS*, *119*(39), 1–7. https://doi.org/10.1073/pnas.2200333119

Kashiwagi, T., Ohlemiller, T. J., & Werner, K. (1987). Effects of external radiant flux and ambient oxygen concentration on nonflaming gasification rates and evolved products of white pine. *Combustion and Flame*, *69*(3), 331–345. https://doi.org/10.1016/0010-2180(87)90125-8

Kravka, M., Krejzar, T., & Cermak, J. (1999). Water content in stem wood of large pine and spruce trees in natural forests in central Sweden. *Agricultural and Forest Meteorology*, *98*, 555–562. https://doi.org/10.1016/s0168-1923(99)00123-9

LANDFIRE, 2020. Existing Vegetation Type Layer, LANDFIRE 2.2.0. *US. Department of Interior, Geological Survey, and U.S. Department of Agriculture.* http://www.landfire/viewer

Larimer County, Larimer County Office of Emergency Management. (2021). *Cameron Peak Fire Risk Assessment.* https://www.larimer.org/sites/default/files/uploads/2021/cpf_risk_assessment_overview_5.24.2021.pdf

Link, T., & Marks, D. (1999). Distributed simulation of snowcover mass- and energy-balance in the boreal forest. *Hydrological Processes*, *13*(14–15), 2439–2452. https://doi.org/10.1002/(SICI)1099-1085(199910)13:14/15<2439::AID-HYP866>3.0.CO;2-1

Maxwell, J. D., Call, A., & St. Clair, S. B. (2019). Wildfire and topography impacts on snow accumulation and retention in montane forests. *Forest Ecology and Management*, *432*, 256–263. https://doi.org/10.1016/j.foreco.2018.09.021

McGrath, D., Zeller, L., Bonnell, R., Reis, W., Kampf, S., Williams, K., Okal, M., Olsen-Mikitowicz, A., Bump, E., Sears, M., & Rittger, K. (2023). Declines in Peak Snow Water Equivalent and Elevated Snowmelt Rates Following the 2020 Cameron Peak Wildfire in Northern Colorado. *Geophysical Research Letters*, *50*(6). https://doi.org/10.1029/2022GL101294

Mock, C. J., & Birkeland, K. W. (2000). Snow Avalanche Climatology of the Western United States Mountain Ranges. *Bulletin of the American Meteorological Society*, *81*(10), 2367–2392. https://doi.org/10.1175/1520-0477(2000)081<2367:sacotw>2.3.co;2

Molotch, N. P., Barnard, D. M., Burns, S. P., & Painter, T. H. (2016). Measuring spatiotemporal variation in snow optical grain size under a subalpine forest canopy using contact spectroscopy. *Water Resources Research*, *52*(9), 7513–7522. https://doi.org/10.1002/2016WR018954

Molotch, N. P., Brooks, P. D., Burns, S. P., Litvak, M., Monson, R. K., McConnell, J. R., & Musselman, K. (2009). Ecohydrological controls on snowmelt partitioning in mixed-conifer sub-alpine forests. *Ecohydrology*, 2(2), 129–142. https://doi.org/10.1002/eco.48

Molotch, N. P., Blanken, P. D., Williams, M. W., Turnipseed, A. A., Monson, R. K., & Margulis, S. A. (2007). Estimating sublimation of intercepted and sub-canopy snow using eddy covariance systems. *Hydrological Processes*, *21*(12), 1567–1575. https://doi.org/10.1002/hyp.6719

Moore, C., Kampf, S., Stone, B., & Richer, E. (2015). A GIS-based method for defining snow zones: application to the western United States. *Geocarto International*, *30*(1), 62–81. https://doi.org/10.1080/10106049.2014.885089

Musselman, K. N., & Pomeroy, J. W. (2017). Estimation of Needleleaf Canopy and Trunk Temperatures and Longwave Contribution to Melting Snow. *Journal of Hydrometeorology*, *18*(2), 555–572. https://doi.org/10.1175/JHM-D-16-0111.1

Pomeroy, J. W., Gray, D. M., Shook, K. R., Toth, B., Essery, R. L. H., Pietroniro, A., Hedstrom, N., Taylor, S., & Hardy, J. (1998). An evaluation of snow accumulation and ablation processes for land surface modelling. *Hydrological Processes*, *12*(15), 2339–2367. https://doi.org/10.1002/(SICI)1099-1085(199812)12:15<2339::AID-HYP800>3.0.CO;2-L

Pomeroy, J. W., Marks, D., Link, T., Ellis, C., Hardy, J., Rowlands, A., & Granger, R. (2009). Impact of coniferous forest temperature on incoming longwave radiation to melting snow. *Hydrological Processes*, *23*(17), 2513–2525. https://doi.org/10.1002/hyp.7325

R Core Team. (2023). R: A language and environment for statistical computing. R Foundation for Statistical Computing, Vienna, Austria. https://www.R-project.org/

Reis, W., McGrath, D., Elder, K., Kampf, S., & Rey, D. (2024). Quantifying Aspect-Dependent Snowpack Response to High-Elevation Wildfire in the Southern Rocky Mountains. *Water Resources Research*, *60*(9). https://doi.org/10.1029/2023WR036539

Richer, E. E., Kampf, S. K., Fassnacht, S. R., & Moore, C. C. (2013). Spatiotemporal index for analyzing controls on snow climatology: Application in the Colorado Front Range. Physical Geography, 34(2), 85–107. https://doi.org/10.1080/02723646.2013.787578

Rouse, W. R. (1984). Microclimate at Arctic Tree Line 1. Radiation Balance of Tundra and Forest. *Water Resources Research*, *20*(1), 57–66. https://doi.org/10.1029/WR020i001p00057

Rutter, N., Essery, R., Baxter, R., Hancock, S., Horton, M., Huntley, B., Reid, T., & Woodward, J. (2023). Canopy Structure and Air Temperature Inversions Impact Simulation of Sub-Canopy Longwave Radiation in Snow-Covered Boreal Forests. *Journal of Geophysical Research. Atmospheres*, *128*(14). https://doi.org/10.1029/2022JD037980

SketchAndCalc. (2024, December 11). *Area Calculator App | Irregular Area Calculator | Calculate Irregular Shape area*. https://www.sketchandcalc.com/

Serreze, M. C., Clark, M. P., Armstrong, R. L., McGinnis, D. A., & Pulwarty, R. S. (1999). Characteristics of the western United States snowpack from snowpack telemetry

(SNOTEL) data. *Water Resources Research*, *35*(7), 2145–2160. https://doi.org/10.1029/1999WR900090

Seyednasrollah, B., & Kumar, M. (2014). Net radiation in a snow-covered discontinuous forest gap for a range of gap sizes and topographic configurations. *Journal of Geophysical Research. Atmospheres*, *119*(17), 10,323-10,342. https://doi.org/10.1002/2014JD021809

Szeitz, A. J., & Moore, R. D. (2023). Modelling snowpack bulk density using snow depth, cumulative degree-days, and climatological predictor variables. *Hydrological Processes*, *37*(1). https://doi.org/10.1002/hyp.14800

Thieurmel, B. & Elmarhraoui, A. (2022). _suncalc: Compute Sun Position, Sunlight Phases, Moon Position and Lunar Phase_. R package version 0.5.1. https://CRAN.R-project.org/package=suncalc

Uecker, T. M., Kaspari, S. D., Musselman, K. N., & Skiles, S. M. (2020). The Post-Wildfire Impact of Burn Severity and Age on Black Carbon Snow Deposition and Implications for Snow Water Resources, Cascade Range, Washington. *Journal of Hydrometeorology*, *21*(8), 1777–1792. https://doi.org/10.1175/JHM-D-20-0010.1

U.S. Department of Agriculture. (2023). *National Agriculture Imagery Program (NAIP) imagery* [Data set]. U.S. Department of Agriculture, Farm Service Agency. https://datagateway.nrcs.usda.gov/

Vorster, A. G. (2020). *Characterizing forest biomass and the impacts of bark beetles and forest management in the Southern Rocky Mountains, USA* [Doctoral dissertation, Colorado State University]. ProQuest Dissertations & Theses

Westerling, A. L. (2016). Increasing western US forest wildfire activity: sensitivity to changes in the timing of spring. *Philosophical Transactions of the Royal Society of London. Series B. Biological Sciences*, *371*(1696), 1–10. https://doi.org/10.1098/rstb.2015.0178

Wiscombe, W. J., & Warren, S. G. (1980). A Model for the Spectral Albedo of Snow. I: Pure Snow. *Journal of the Atmospheric Sciences*, *37*(12), 2712–2733. https://doi.org/10.1175/1520-0469(1980)037<2712:AMFTSA>2.0.CO;2

APPENDICES

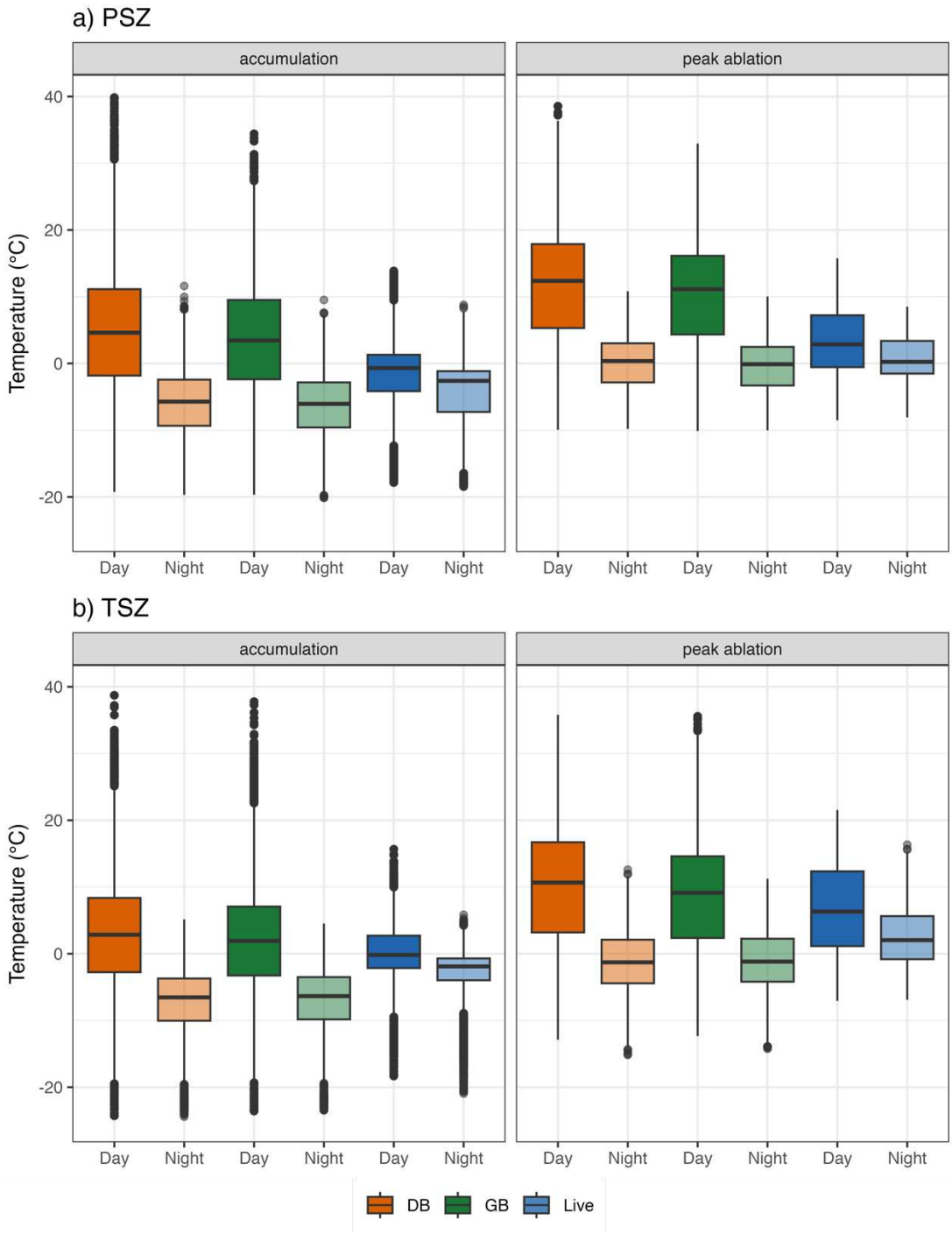

Figure A1. Boxplot of day and night temperature values by burn condition in a) persistent snow zone (PSZ) and b) transitional snow zone (TSZ) from the accumulation period (2 February–peak ablation period) and the peak ablation period (when SWE and snow depth continuously decreased and well diameters increased consistently from day to day – the snow-free date of each burned site).

Table A1. Standard deviation of replicate dead-burn (DB), green-burn (GB) and live sensors, by aspect in the persistent (PSZ) and transitional (TSZ) snow zones, for the period from 2 February–the respective snow-free date of each zone.

Zone	Burn Condition	Standard Deviation (°C)	
		North Aspect Sensors	South Aspect Sensors
PSZ	DB	0.6	1.6
	GB	0.9	2.2
	live	0.7	0.6
TSZ	DB	0.6	1.0
	GB	0.7	1.3
	live	0.4	0.4

Appendix B. Melt Volume Comparison

Table B1. Mean percent difference between open and tree area snow water equivalent (SWE) (cm) of the persistent (PSZ) and transitional (TSZ) snow zones during accumulation and peak ablation for all four observed trees per zone, including green-burn (GB) and dead-burn (DB) burn conditions.

Zone	Tree ID	Burn Condition	Mean SWE % Difference Accumulation	Mean SWE % Difference Peak Ablation
PSZ	1	GB	32.5	54.2
	2	GB	14.9	39.3
	3	GB	14.2	36.2
	4	DB	13.8	26.1
TSZ	1	GB	4.9	38.5
	2	GB	4.8	38.2
	3	GB	4.7	37.6
	4	DB	4.9	37.2

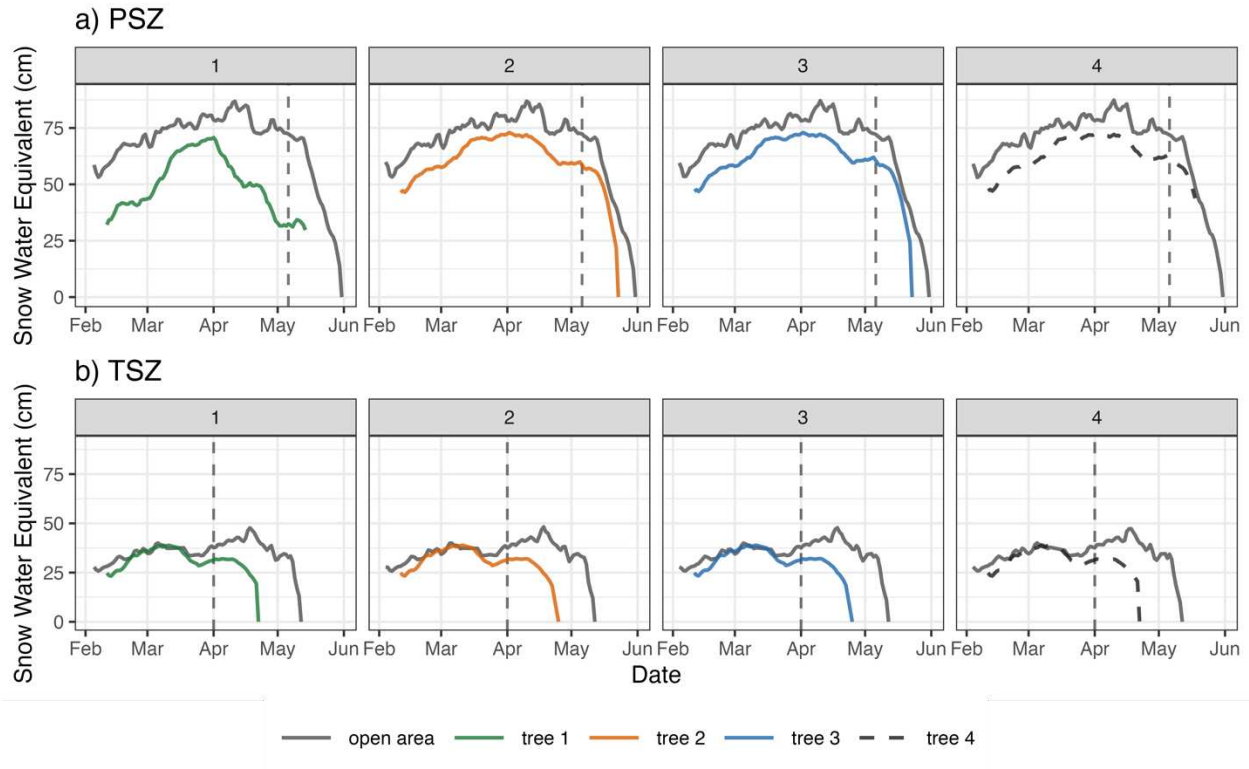

Figure B1. Rate of change of snow water equivalent (SWE) between open and tree areas for the entire period of observation in the persistent (PSZ) and transitional (TSZ) snow zones. The vertical dashed line represents the beginning of the peak ablation period. Note that tree 4 is a dashed black line because it is a dead-burn tree, while trees 1–3 are green-burn trees in both plots a) and b).